Early Cambrian tidal sedimentary environments, western Victoria Island, Arctic Canada

By
Andrew Michael Durbano

A Thesis Submitted to the College of Graduate Studies and Research in Partial Fulfillment of the Requirements for the Degree of Master of Science in the Department of Geological Sciences
University of Saskatchewan
Saskatoon

PERMISSION TO USE

In presenting this thesis in partial fulfillment of the requirements for a Postgraduate degree from the University of Saskatchewan, I agree that the Libraries of this University may make it freely available for inspection. I further agree that permission for copying of this thesis in any manner, in whole or in part, for scholarly purposes may be granted by the professor or professors who supervised my thesis work or, in their absence, by the Head of the Department or the Dean of the College in which my thesis work was done. It is understood that any copying or publication or use of this thesis or parts thereof for financial gain shall not be allowed without my written permission. It is also understood that due recognition shall be given to me and to the University of Saskatchewan in any scholarly use which may be made of any material in my thesis.

Requests for permission to copy or to make other use of material in this thesis in whole or part should be addressed to:

Head of the Department of Geological Sciences

University of Saskatchewan

Saskatoon, Saskatchewan Canada S7N 5E2

OR

Dean

College of Graduate Studies and Research

University of Saskatchewan

107 Administration Place

Saskatoon, Saskatchewan Canada S7N 5A2

ABSTRACT

The currently unnamed early Cambrian (Series 2, Stage 4) sandstone unit is exposed in the Minto Inlier of western Victoria Island, Canadian Arctic Islands, and forms the base of the Phanerozoic succession. Coeval with other sandstones of this age in Laurentia, it was deposited in a shallow-marine embayment on the passive margin during the initial phase of the early Paleozoic transgression. Four facies associations are recognized: (1) outer embayment sand dune complex characterized by laterally continuous, planar cross-stratified, medium- to coarse-grained sandstone; (2) inner embayment sand flat consisting dominantly of fine- to medium-grained bioturbated sandstone and fine- to medium-grained sandstone interbedded with laminated mudstone; (3) coastal lagoon characterized by laterally continuous, medium-grained oolitic ironstone and fine- to medium-grained bioturbated sandstone; and (4) offshore muddy shelf consisting dominantly of laminated mudstone with discontinuous seams of medium- to coarse sand. Bioturbation in the form of a typical early Cambrian suite of shallow-subtidal ichnofossils predominated in the inner embayment and coastal lagoon settings, representing a low-diversity *Cruziana* ichnofacies. Oolitic ironstone horizons in the coastal lagoon setting mark periods of low sedimentation rates when iron became concentrated and calcite was the primary cementing agent. Dunes are, for the most part, non-bioturbated or contain just a few individual burrows belonging to *Skolithos*, representing the *Skolithos* ichnofacies. The dominantly tabular, sheet-like geometry of the sandstones characterizes a comparatively lower energy regime than what has been found in typical complex dune geometries in modern and ancient examples and is attributed to sediment deposition under essentially uniform current speeds at consistent

water depth conditions on a low-gradient shelf. Paleocurrent measurements and thickness variation suggest that deposition was affected by undulating topography on the Proterozoic basement within facies association 1 and 2, as well as by syndepositional faulting in some areas. The coastline is envisaged as a complex of bays and lagoons. The embayment opened to the northwest where sandbars developed offshore; stratigraphic thinning towards both the south and northeast indicates the direction of the paleoshoreline. Approximately shoreline orthogonal paleocurrents are considered indicative of a tidal origin. The lack of hummocky cross-stratification suggests there was no influence of major storms in this region.

ACKNOWLEDGEMENTS

I would like to thank my supervisor Dr. Brian Pratt for providing me with the opportunity to study this exciting topic and also for his patience with slow but steady progress. Funding was provided by Natural Resources Canada's Geo mapping for Energy and Minerals (GEM) program and a Natural Sciences and Engineering Research Council (NSERC) Research Affiliate Program (RAP) bursary awarded to A. Durbano. I would also like to give a personal thank you to Dr. Gabriela Mángano for her help with trace fossils and facies analysis and Dr. Luis Buatois for his help with facies analysis and sequence stratigraphy.

For all of their support and discussions, both in and out of the field, I am grateful to colleagues Dr. Thomas Hadlari and Dr. Keith Dewing at the Geological Survey of Canada. Both of you always found time to answer my e-mails, meet with me when I was in Calgary and one of you even let me live in your house for a week while I was writing this manuscript (thanks Thomas!). Jordan Mathieu is thanked for his assistance in the field.

Finally, I want to thank my family and friends for their support and words of encouragement during an interesting period of my life.

TABLE OF CONTENTS

1. Introduction

In comparison to younger rocks of a similar setting, Early Cambrian shallow-marine settings on the continental shelves of a number of cratons are unique transgressive environments that led to the deposition of vast amounts of compositionally mature sand (Dalrymple et al., 1985; Cant and Hein, 1986; Simpson and Eriksson, 1990; McKie, 1993; MacNaughton et al., 1997; Desjardins et al., 2010a, 2012a, b). Thermal subsidence of the passive margin along these continental margins associated with the protracted breakup of the supercontinent Rodinia during the late Neoproterozoic led to a global rise in sea level and created the necessary accommodation space (e.g., Bond and Kominz, 1984; Levy and Christie-Blick, 1991). The absence of land plants before the Silurian promoted the development of extensive subaerial dune fields and braided fluvial systems on land (Dalrymple et al., 1985; MacNaughton et al., 1997; Rainbird et al., 1997; Long and Yip, 2009). Large amounts of siliciclastic sediment stored on the land surface of the continental interiors were carried to the continental shelf by fluvial systems and by the flooding and ravinement of pre-existing sandy coastal deposits during the transgression, establishing these shallow seas as the sandiest of the Phanerozoic. The facies present evidence for a combination of variably strong tidal action and subordinate storm processes (Desjardins et al., 2012a, b).

Early Cambrian sandstones mantle much of the margin of the North American craton, called Laurentia, and they comprise the basal part of the Sauk Megasequence. Examples include the Gog Group of the southern Rocky Mountains of western Canada

(Desjardins, 2010b, 2012b), the Backbone Ranges Formation in the Mackenzie Mountains (MacNaughton et al., 1997), the Bradore Formation in southern Labrador (Long and Yip, 2009), the Chillowee Group in Virginia (Simpson and Eriksson, 1990), the Hardyston Formation in Pennsylvania (Simpson et al., 2002), the Zabriskie Quartzite in Death Valley (Prave, 1991), and the Eriboll Sandstone in Scotland (McKie, 1990), the last of which is part of a crustal fragment of East Laurentia (Cawood et al., 2007). Continued rise in global sea level meant that these sandstones were time-transgressive, which led to shallow-marine sandstones of middle and late Cambrian age in the craton interiors, such as the Flathead Formation in western Laurentia, the Mt. Simon Formation of the mid-continent and the Potsdam Formation of the St. Lawrence Lowlands (Lochman-Balk, 1971**;** Driese et al., 1980**;** Runkel et al., 2008**;** Sanford and Arnott, 2009).

The nature of the Cambrian transgression in Arctic Laurentia is not well known, in part because of the lack of exposure and also because the most outboard deposits are more or less absent (Dewing and Nowlan, 2012). Early Paleozoic rocks are widely distributed on Victoria Island of the western Arctic where they have been mapped at a regional scale. Here, I present a detailed study of the sedimentology of the currently unnamed lower Cambrian sandstone unit exposed around the head of Minto Inlet in the western part of the island (Figure 1). This allows a reconstruction of the depositional setting and a comparison to its counterparts elsewhere in Laurentia. Documenting the unnamed sandstone helps write a missing chapter in the Cambrian stratigraphy of the Canadian Arctic Islands.

2. Geologic setting

Ancestral North America formed from the amalgamation of Archean cratons, including the Slave, Churchill, and Superior provinces, during Paleoproterozoic collisional events recorded by orogenic belts (Hoffman, 1988). Grenvillian orogenesis along (present-day) southeastern North America contributed to the formation of the supercontinent Rodinia during the Mesoproterozoic era (Davidson, 2008). Rodinia broke up during the late Neoproterozoic and the core of present-day Laurentia includes Greenland but excludes terranes that may have existed offshore along eastern and western North America. By Cambrian time northern Laurentia was bordered by passive margins on its present-day north, east, and west (e.g., Hadlari et al., 2012).

Neoproterozoic rifting probably began at the Gunbarrel magmatic event ca. 780 Ma along the western margin of the Laurentian craton (Harlan et al., 2003). Franklin dikes and flood basalts of the Natkusiak Formation along the Franklinian margin of the Canadian Arctic Islands mark the onset of rifting along the northwestern Laurentian margin at about 723 Ma (Heaman et al., 1992; Rainbird et al., 1998). The Franklin dike swarm is known to extend as far as northern Greenland (Denyszyn et al., 2006). However, sedimentary rocks recording the early phase of passive margin development, correlative with the Windermere Supergroup of the western margin of Laurentia (Ross, 1991), are exposed only sporadically in the Franklinian basin (Trettin, 1991; Harrison, 1995; Dewing et al., 2004).

Early Cambrian strata of the Ellesmere Group were deposited in an open-marine shelf around and below wave base with progradation of the prodeltaic front towards the shelf-edge and deepwater basin while accommodation space was filled by sediment (Dewing et al., 2008). Similarly, the Lower Cambrian Gog Group overlies the Windermere Supergroup in the southern Rocky Mountains and represents deposits of a passive margin in shallow subtidal, inner-shelf, and tidal-flat environments (Desjardins et al., 2010a, b, 2012a, b). Within the Gog Group of the central Rocky Mountains, the McNaughton Formation consists of fluvial sediments that accumulated in half-grabens that were active during the latest Neoroterozoic to early Cambrian, representing the final stage of rifting on the passive continental margin (Lickorish and Simony, 1995). In the Arctic Islands, subsequent transgression across the platform curtailed terrigenous sediment transport and led to deposition of platformal carbonates from the middle Cambrian through Silurian time (Trettin et al., 1991). Similarly, all along the shelf-slope break and shelf interior of western Laurentia there developed a series of stacked carbonate platforms (Aitken, 1993, 1997; Pratt, 2002).

The Mackenzie Mountains of mainland Northwest Territories are located inboard of what was the subsiding continental shelf margin in Cambrian time, characterized by paleotopography probably inherited from Neoproterozoic rifting (Maclean, 2011) and recording a thick wedge of sediment consisting of a series of unconformity-bounded, westward-prograding strata (MacNaughton et al., 2000). The wedge consists of Neoproterozoic rocks overlain by extensive braid-delta deposits ranging from braidplain to distal prodelta facies in the northwest (MacNaughton et al., 1997). These deposits

pass upward into proximal basin, slope, and shelf carbonates of late early Cambrian age belonging to the Sekwi Formation (Dilliard et al., 2010). Early Cambrian syndepositional 'down-to-basin' faulting during deposition of the lower Sekwi Formation increased accommodation basinward and was most likely a continuation of extension that began during the latest Neoproterozoic rifting of western Laurentia (Dilliard et al., 2010). Faulting continued locally into the middle Cambrian (Kimmig and Pratt, in press). Northwards, the early Paleozoic margin is fragmented and buried north of the Mackenzie Mountains under the Mackenzie River delta and Beaufort Sea, presumably it made a sharp bend somewhere in the present-day offshore before trending more or less northeast; the margin appears to have made another orthogonal bend in the area of Melville and Prince Patrick islands, before trending again northeast to northern Ellesmere Island and North Greenland (Hadlari, 2013).

On mainland Northwest Territories an eastward transgression accompanied subsidence, which resulted in early and middle Cambrian strata, i.e., sandstone of the Mount Clark Formation, shales of the Mount Cap Formation, and evaporitic facies of the Saline River Formation (Hadlari et al., 2012; MacNaughton et al., 2013), directly overlying pre-Windermere Proterozoic rocks in the Northern interior plains (Cook and Maclean, 2004). These rocks were deposited in a semi-enclosed epicontinental marine basin, exhibiting variable thickness and distribution that define abundant paleotopographic highs and lows (Dixon and Stasiuk, 1998; Maclean, 2011). The sub-Cambrian unconformity represents a large gap in time, with trilobites belonging to the *Bonnia–Olenellus* Biozone present close to the unconformity surface in the lower part of

the Mount Cap Formation (Aitken et al., 1973; MacNaughton et al., 2013), while in the Mackenzie Mountains fossils belonging to the older *Nevadella* Biozone occur in the lower Sekwi Formation (Fritz, 1972, 1973; Aitken, 1993) (Figure 2). On northeastern Ellesmere Island the Rawlings Bay Formation is considered equivalent to the Dallas Bugt Formation on Bache Peninsula and south of Richardson Bay on Inglefield Land and the upper part of the sandstone-dominated unit of the Buen Formation in North Greenland (Dewing et al., 2008). Trace and body fossils from the Buen Formation are early Cambrian in age (Ineson and Peel, 1997). The Kane Basin Formation contains trilobites from the medial *Bonnia–Olenellus* Biozone (Dewing et al., 2008) and correlates to the recessive, upper part of the Buen Formation and the Marshall Bugt Member of the Dallas Bugt Formation (Peel et al., 1982; Dewing et al., 2008).

3. Previous work

There are two physiographic regions on Victoria Island. The Shaler Mountains run diagonally across the centre of the island and are cored by Neoproterozoic sedimentary and igneous rocks of the Shaler Supergroup comprising the Minto Inlier (Rainbird, 1993; Rainbird et al., 1996, 2010; Bédard et al., 2012). The Shaler Supergroup consists predominantly of shallow-water carbonates, with subordinate sandstone, mudstone and gypsum deposited in a shallow-water intra-continental basin (Thomson et al., 2014). Overlying flood basalts of the Natkusiak Formation are attributed to mantle plume-related volcanism (Heaman et al., 1992). To the northwest and southeast are lowlands underlain by flat-lying to gently dipping lower Paleozoic platformal strata which unconformably overlie the Shaler Supergroup and Archean

rocks and range in age from early Cambrian to Late Devonian (Thorsteinsson and Tozer, 1962; Dewing et al., 2013).

The base of the Paleozoic succession consists of unnamed siliciclastic strata previously described by Thorsteinsson and Tozer (1962) as Map Unit 10a (Cambrian, 360–400 ft [110–122 m]). They noted that it consists of fine-grained, thinly bedded green and red sandstone with thin beds of red, green and grey siltstone and shale, and medium-grained, thinly bedded glauconitic sandstone. Sediment provenance appears to be a mixture of relatively local sources, with detrital zircon ages including the Shaler Supergroup, Slave craton, Taltson-Thelon orogen, and Wopmay orogen (Hadlari et al., 2012).

These siliciclastic strata (currently informally referred to as the Cambrian 'clastic unit') are overlain by the informally termed Cambrian 'tan dolostone' and 'stripy' units, followed by the Cambro-Ordovician Victoria Island Formation (Dewing et al., 2013). The tan dolostone unit consists of light-brown mudstone to grainstone with locally developed thrombolite mounds. The stripy unit contains thin- to medium-bedded red mudstone and shale intercalated with green, grey and red dolomudstone. The Victoria Island Formation is made up of light-grey, fine- to coarsely crystalline, fabric-destructive dolostone with abundant silicification in the upper two-thirds of the unit. These are overlain by carbonates of Late Ordovician to Late Devonian in age (Dewing et al., 2013).

The clastic unit is correlative temporally and lithologically to the basal shallow subtidal sandstones of the Gog Group that mark the initiation of transgression in the southern Rocky Mountains. The studied area of Victoria Island, however, never experienced the degree of subsidence and corresponding large, but fluctuating, sediment supply of the Gog Group (Desjardins et al., 2010a, 2012a, b). No maximum flooding surfaces and subsequent progradational sequences like those in the Gog Group are present in the clastic unit. Dixon and Stasiuk (1998) inferred a maximum flooding surface separating sandstones of the Mount Clark Formation from the mudstone-dominated Mount Cap Formation based on the change in style of deposition. In the Mackenzie River valley area, the lower Mount Cap Formation is within the *Bonnia–Olenellus* Biozone and is therefore correlative with the upper part of the clastic unit. In the western Mackenzie Mountains, however, at least the upper part of the Mount Clark Formation correlates with the clastic unit and trilobite biostratigraphy indicates that the base of the Mount Cap Formation (MacNaughton et al., 2013) is correlative to the lower part of the tan dolostone unit (Figure 2). Likewise sandstones of the Gog Group are overlain first by mixed carbonate–siliciclastic deposits followed by the regionally extensive carbonate platform represented by the Cathedral Formation. The shift to carbonate-dominated deposition is recorded all over Laurentia and is presumably related to a waning of siliciclastic sediment supply to the outer shelf region as transgression progressed towards the cratonic interior.

4. Methods

The unnamed lower Cambrian clastic unit is divided here into eleven distinct facies (Table 1). Four outcrop sections and one drill core were measured (Figure 3; Table 2). Facies are based on lithology, sedimentary structures, and bedding geometry, along with discernible trace fossils and bioturbation intensity (BI index). The facies descriptions follow the terminology of Taylor and Goldring (1993) for bioturbation, and of Ashley (1990) for subaqueous bedforms. The facies are grouped into four associations (FAs).

Table 2: Location of measured sections and drill core.

Section	Latitude	Longitude
Drill core		
Section A (GNME 07-04)	71° 44.685'N	113° 44.101'W
Measured Sections		
Section B	71° 36.877'N	115° 15.193'W
Section C	71° 26.152'N	115° 26.280'W
Section D	71° 24.316'N	115° 48.233'W
Section E	71° 61.404'N	115° 25.017'W

5. Results

Table 1: Facies in the unnamed clastic unit, Victoria Island.

Facies	Lithology and sedimentary structures	Depositional processes	Fossils, ichnogenera and bioturbation index (BI)	Distribution
Ms Mudstone	0.5–2 cm thick, thinly laminated micaceous mudstone; locally silty to sandy; locally contains discontinuous seams of medium- to coarse sand; preserved mudstone intervals can reach up to 2 m thick.	low energy, suspension fall-out.	*Planolites*, olenelloid trilobite sclerites. BI=0–1	FA-2, FA-4
Sm Massive	10–150 cm thick, well-sorted, fine- to coarse-grained	Low to moderate energy; bed-	No recognizable bioturbation	FA-2, FA-3,

sandstone	sandstone; appears structureless. Locally contains abundant pebbles and 2–20 cm clasts of dolostone, red weathering.	load deposition under low-flow regime. Massive nature probably related to uniformity in grain size.		FA-4
He Lenticular- and wavy-bedded sandstone	2–20 cm thick, well-sorted, fine- to medium-grained sandstone; interbedded with 0.5–20 cm thick, thinly laminated mudstone. Local plane and ripple cross-lamination, mud drapes in sandstone. Preserved in 20–50 cm intervals.	Low energy; suspension fallout and episodic sand deposition. Type of bedding related to the alternation of current or wave action and slack-water periods.	*Rusophycus*, *Planolites*, *Skolithos*, *Cruziana*, *Arenicolites*, *Palaeophycus*, *Thalassinoides*, ?*Teichichnus*. BI=1–2	FA-2, FA-4
Sw Wave-rippled sandstone	Lenticular to wavy beds, 1–10 cm thick, well-sorted, fine-grained sandstone.	Low- to moderate-energy; bed-load deposition of small bedforms.	*Planolites*, *Skolithos*, *Diplocraterion*. BI=1–2	FA-2
S_{B1} + S_{B2} Bioturbated sandstone	Bioturbated, moderate- to well-sorted, fine- to coarse-grained sandstone. Primary sedimentary structures unrecognizable or absent. In Section A glauconite is commonly found in burrows and around mud drapes. S_{B1}: Heterolithic, 2–50 cm thick, moderate- to well-sorted, fine- to medium-grained argillaceous sandstone; mud drapes, trace mudstone due to bioturbation. Recessive weathering, fissile sandstone. S_{B2}: 5–50 cm thick, moderate- to well- sorted, fine- to coarse-grained sandstone; mud drapes. Locally wave-rippled, contains synsedimentary dykelets (syneresis cracks). Locally preserved cross-stratification, plane-lamination.	Episodic sand deposition in low-energy areas of the inner shelf and colonization mainly by a deposit feeding fauna.	S_{B1}: ?*Teichichnus*, *Trichophycus*, *Skolithos*, *Thalassinoides*, *Planolites*, *Rosselia*. BI=2–3 S_{B2}: *Skolithos*, *Arenicolites*, *Rusophycus*, *Diplocraterion*, *Palaeophycus*, *Phycodes,* ?*Teichichnus*, ?*Helminthopsis*. BI=1–3	S_{B1}: FA-2, FA-3 S_{B2}: FA-2, FA-3
S_L Plane-laminated sandstone	5–10 cm thick, moderate- to well- sorted, fine- to medium-grained, plane-laminated sandstone.	Low- to moderate-energy; bed-load deposition under lower flow regime.	*Diplocraterion*, *Skolithos*, *Planolites*, *Palaeophycus*. BI=1–2	FA-2, FA-4
Sp_1 + Sp_2 + Sp_3 Planar cross-stratified sandstone	Tabular bodies, locally scoured, planar and low-angle cross-stratified, moderate- to well- sorted, fine- to coarse-grained sandstone. Sp_1: 5–60 cm thick, sharp-	Moderate- to high-energy; bed-load deposition of 2-D dunes.	Sp_1: No recognizable bioturbation Sp_2: *Skolithos*, and *Palaeophycus* associated with overlying bioturbated sandstones are locally	Sp_1: FA-1, FA-2 Sp_2: FA-1

	based, well-sorted, fine- to medium-grained sandstone; Locally contains opposing foreset directions, ripple-tops. Sp_2: 20–140 cm thick, sharp-based, moderate- to well-sorted, medium- to coarse-grained, locally fine-grained sandstone; Locally 150–300 cm thick with scoured bases. Coarse sandstone commonly drapes the foresets, Local reactivation surfaces, herringbone cross-bedding, ripple-tops. Sp_3: 15–140 cm thick, sharp based, moderate- to well-sorted, medium- to coarse-grained sandstone; Conglomeritic, clasts 1–5 cm, abundant de-watering structures.		present BI=0–1 Sp_3: No recognizable bioturbation	Sp_3: FA-1
S_o Oolitic ironstone	5–40 cm thick, moderate- to well- sorted, fine- to medium-grained, ooidal ironstone; locally cross- laminated, locally preseved in intervals reaching 3 m.	Low energy; suspension fallout and episodic sand deposition with abundant Fe	No recognizable bioturbation	FA-3

5.1. Facies association 1: outer embayment sand dune complex

5.1.1. Description

This facies association is characterized by laterally continuous, 20–140 cm thick, planar cross-stratified, medium- to coarse-grained sandstone (Sp_2). Reactivation surfaces, ripple-tops and eroded, convex-upward foreset tops are locally preserved (see Figure 4). Stacked beds with opposing foreset directions are also present in places (Figure 4a). Beds of Sp_2 are locally separated by laminated mudstone (Ms), 2–10 cm thick, fine- to medium-grained sandstone interbedded with 0.5–20 cm thick laminated mudstone (He) (Figure 6c), 1–10 cm thick, plane-laminated, fine- to medium-grained

sandstone (S_L) and 10–20 cm thick, well-sorted, fine-grained massive sandstone (Sm). No wave-formed structures were observed.

Facies Sp_1 is less common than Sp_2, has a bed thickness of 5–60 cm and consists of planar cross-stratified, fine- to medium-grained sandstone. Reactivation surfaces and eroded, convex-upward foreset tops are scarce (Figure 4e). Section C contains 15–140 cm thick, medium- to coarse-grained conglomeritic (clasts 5–30 mm) planar cross-stratified sandstones with abundant, conical dewatering pipes (Sp_3) (see Figure 4b,d) that mantles a paleokarst surface on underlying Neoproterozoic carbonate rocks (Mathieu et al., 2013).

Facies Sp_2 is present at all studied locations except for Section E and crops out elsewhere in western Victoria Island. Bedset thickness ranges from 5.5 m to 6.5 m and forms sheet-like geometries that extend laterally 100 m or more (see Figures 9 and 10). Grain size exhibits a uniform to faintly coarsening-upward trend. The lower bounding surfaces are flat but locally are marked by shallow depressions up to 0.3 m deep. Locally, large cross-stratified beds in outcrop reach 3 m in thickness, exhibiting scoured bases and lacking a sheet-like geometry (Figure 5). Facies Sp_1 and Sp_3 also contain flat lower bounding surfaces but Sp_3 is only found locally, whereas facies Sp_1 dominates the lower part of Section B. The lateral continuity and possibility of a sheet-like geometry for facies Sp_1 and Sp_3 are unknown but beds extend laterally 10's of meters in outcrop. The preserved style of cross-stratification in facies Sp_1, Sp_2 and Sp_3 is simple (sensu Ashley,

1990), with inclined foresets that sporadically contain discontinuities that are reactivation surfaces. Mudstone drapes are rare or absent.

Bioturbation is uncommon (BI 0–1) and trace fossils are predominantly vertical burrows belonging to *Skolithos*. Simple horizontal forms assigned to *Palaeophycus* and arthropod scratch marks are occasionally preserved at the tops of beds that are overlain by bioturbated sandstones belonging to Facies S_{B2}.

5.1.2. Interpretation

Planar cross-stratified sandstone associated with bioturbation was deposited by 2-D bedforms in a tide-dominated outer embayment sand dune complex. The variation in scale of cross-stratification is interpreted as the product of the migration of subtidal dunes of varying size (Berné et al. 1993**;** Yoshida et al. 2004**;** Sixsmith et al. 2008**;** Desjardins et al. 2012a**;** Pearson et al., 2013). The textural maturity, abundance of medium- to large-scale cross-stratification, stacked beds with opposing foreset directions and rare mudstone drapes imply deposition in a dominantly high-energy, subtidal setting characterized by active dune migration alternating with periods of reduced sedimentation and energy (Pollard et al. 1993; Yoshida et al. 2004). These conditions kept fine-grained particles in suspension, leading to a low proportion of mudstone. The low bioturbation index suggests a shifting sandy substrate under high-energy conditions that prevented the development of colonization windows (Pemberton et al., 1992; MacEachern and Bann, 2008; Desjardins et al., 2010b).

The predominant simple bedform geometry (sensu Ashley, 1990) is similar to Type I cross-stratification of Allen (1980), and characterizes a comparatively lower energy regime than what has been found in typical complex dune geometries in modern and ancient examples (e.g. Yoshida et al., 2004; Desjardins et al., 2012a). Laterally continuous planar bedform geometry is attributed to sediment deposition under uniform tidal current speeds in consistent water depths on a low-gradient seafloor where sands did not aggrade vertically but prograded laterally with little interruption. Local, concave-upward reactivation surfaces suggest periods of strong erosion on the lee side (Nio and Yang, 1991). Rare occurrences of more complex geometry are likely due to infilling of tidal channels unrelated to dune migration, or local scouring during higher energy conditions.

5.2. Facies association 2: inner embayment sand flat

5.2.1. Description

This facies association is characterized by 2–50 cm thick, fine- to medium-grained bioturbated sandstone (S_{B1} and S_{B2}) and 2–20 cm thick, fine- to medium-grained sandstone that is interbedded with 0.5–2 cm thick beds of laminated mudstone (He). This facies comprises intervals 20–50 cm thick. Primary stratification is obscured by biogenic reworking, and relict medium-scale cross-stratification is rarely preserved. Mud drapes are abundant and glauconite is locally present around mud drapes and in burrows. Other facies include 1–10 cm thick, fine- to medium-grained, plane-laminated sandstone (S_L) (Figure 6d), 5–60 cm thick, fine- to medium-grained, planar cross-

stratified sandstone (Sp_1), and rare 1–10 cm thick, fine- to medium-grained, wave-rippled sandstone (Sw) (Figure 6b). Laminated mudstone (Ms) is 0.5–2 cm thick, micaceous and locally silty to sandy. At Sections A and C, 30–150 cm thick, fine- to coarse-grained, massive sandstone (Sm) with 2–20 cm clasts of Neoproterozoic dolostone and abundant pebbles mark the base of the succession (Figure 6a).

Bioturbated sandstones (S_{B1} and S_{B2}) are present in all sections and most outcrops in the study region. In well exposed areas they exhibit planar sheet-like geometries that extend laterally 100 m or more (see Figures 9 and 10). Facies He is laterally continuous in association with facies S_{B1} and S_{B2} but also pinches out. Facies Sw is rare and cannot be traced laterally with confidence beyond a few meters. The lateral continuity of facies Sm, S_L and Ms is unknown but they extend laterally at least 10's of meters in outcrop.

Bioturbation is widespread (BI 0–3) and ichnofossils include forms belonging to *Skolithos*, *Arenicolites*, *Diplocraterion*, *Palaeophycus*, *Planolites*, ?*Teichichnus*, *Phycodes*, *Rosselia*, *Trichophycus*, *Rusophycus* (including *R. jenningsi*), *Cruziana*, ?*Helminthopsis*, *Thalassinoides*, and arthropod scratch marks (see Figure 7).

5.2.2. Interpretation

Planar, bioturbated, sheet-like sandstones and associated mudstone was deposited on sand flats in a shallow subtidal inner embayment setting. Dominantly heterolithic facies in this association reflect a more protected inshore environment,

where concentrations of suspended load occur near the turbidity maximum (Johnson and Levell, 1995; Yoshida et al., 2004). Evidence of tides is not apparent due to the lack of preserved primary physical structures. The presence of Sp_1 indicates currents were still important but less pronounced, and scarce wave-ripples show that wave-induced current action was rarely preserved. Bioturbation by a combination of filter- and deposit-feeding fauna indicates prolonged periods of dune inactivity and suspension fall-out in a fully marine environment (Desjardins et al., 2010b). The bioturbated and mud-rich facies suggests longer colonization windows at the sediment-water interface in a low energy sand flat. Facies He and intervals of Ms reflect a more restricted area of the embayment where water turbidity was low. The lack of diminution in trace fossil size in this association does not favour the development of widespread brackish water areas or fluctuating salinity conditions that impart ecological stresses on the trace makers (Gingras et al., 1999; MacEachern and Gingras, 2007) although the BI of 0–1 for facies Ms suggests there may have been local changes in salinity in more restricted areas of the sand flat. Periods of suspension deposition are consistent with the amount of bioturbation seen in terms of current strength and mobility of the substrate.

5.3. Facies association 3: coastal lagoon

5.3.1. Description

This facies association is characterized by laterally continuous, 5–40 cm thick, medium-grained oolitic ironstone (S_O) and 5–50 cm thick and fine- to medium-grained bioturbated sandstone (S_{B1} and S_{B2}). 1–10 cm thick, fine- to medium-grained, plane-

laminated sandstone (S_L) occurs locally. At Section D intervals of S_O reach 3 m in thickness and some beds are cross-stratified. Bioturbation is widespread (BI 0–3) but facies S_O itself contains no discernible bioturbation.

The oolitic ironstone texture is a sandy grainstone to bioclastic sandstone, dominated by quartz grains in a calcite matrix. Allochems include ooids, peloids, and bioclasts of abraded linguliformean (phosphatic) brachiopod valve fragments and pelmatozoan ossicles. The ooids are well-sorted with a spherical to ellipsoidal shape. Quartz grains are well-sorted, sub-rounded to well-rounded and medium-grained. The quartz grains, ooids and peloids have a diameter of 0.1–0.5 mm (Figure 8). The primary iron component is hematite coatings, which is consistent with Clinton-type ironstones (mid-Silurian) located in the Appalachian area of the United States (Cotter and Link, 1993; Gross, 1995).

5.3.2. Interpretation

Oolitic ironstone, bioturbated, planar-bedded, sheet-like sandstones and associated plane-laminated sandstone were deposited in a coastal lagoon. Primary physical structures are obscured by bioturbation in facies S_{B1} and S_{B2} but the local occurrence of cross-stratification in facies S_O indicates currents are still active but less pronounced. Bioturbation by a mainly deposit-feeding fauna indicates prolonged periods of dune inactivity and suspension fall-out that promoted longer colonization windows in a fully marine lower energy setting. Presence of oolitic ironstone horizons with no discernible bioturbation record prolonged periods of low sedimentation rates during

stillstands (Maynard and Van Houten, 1992) in a nearshore lagoonal environment (Bayer, 1989; Young, 1992; Gross, 1995), where iron accumulated. Populations of brachiopods and pelmatozoans developed during episodes of relative quiescence and mud accumulation. However, intermittent higher energy conditions promoted winnowing of the muds and incorporated bioclasts with iron coated quartz grains. The source of iron in the ironstones was probably from lateritic weathering (Young, 1989; Kimberley, 1994; Van Houten, 2000), where warm, humid conditions promoted chemical weathering, in this case, of the widespread Franklin basalts and sills that cover the island. Hematite rimming of quartz grains is suggestive of syndepositional influx of iron (Kearsley, 1989) while the rare occurrence of cross-stratification indicates that locally the ferruginous allochems and sand grains were reworked by waves (e.g. Teyssen et al., 1984; Chafetz et al., 1986).

5.4. Facies association 4: offshore muddy shelf

5.4.1. Description

This facies association is characterized by 0.5–2 cm thick, laminated mudstone (Ms) with discontinuous seams of medium- to coarse sand, preserved in intervals that can reach up to 2 m and contain olenelloid trilobite sclerites belonging to the *Bonnia–Olenellus* Biozone (upper lower Cambrian, series 2, stage 4) (Hadlari et al., 2012; Dewing et al., 2013). Locally, 40–60 cm thick, medium-grained, moderate- to well-sorted massive sandstone (Sm), 1–10 cm thick, fine- to medium-grained, plane-laminated

sandstone (S_L) and 20–50 cm thick intervals of 2–10 cm thick, fine- to medium-grained sandstone interbedded with 0.5–20 cm thick laminated mudstone (He) are present.

Bioturbation in associated sandstones is moderate (BI 1–2) and ichnofossils include forms belonging to *Palaeophycus*, *Planolites*, and *Arenicolites*.

5.4.2. Interpretation

Laminated mudstone and associated massive, lenticular and plane-laminated sandstones at the top of the succession record a transition to an offshore muddy shelf environment. The mudstones are regionally widespread, suggesting that they were deposited farther offshore rather than in a interior, protected part of the sand flat. Evidence of tides is not present in this facies association. Bioturbation by a combination of filter- and deposit-feeding fauna in associated sandstones of facies He indicate periods of suspension fall-out in a fully marine environment. Occasional storms that generated sediment plumes probably account for the sand lenses in facies He and seams of sand in Ms.

6. Sedimentary geometry

Two photomosaics were prepared at Section B where the meandering river cut allows views of the same succession at more or less right angles to each other (Figures 9 and 10).

The contact between FA1 and FA2 is marked by planar cross-stratified sandstones (Sp_2) overlying bioturbated sandstones (S_{B1} and S_{B2}). Following deposition of medium-bedded Sp_2 and overlying facies He over S_{B1} and S_{B2} the right side of the mosaic records a scoured channel that is subsequently infilled by a medium-bedded Sp_2 that migrates in the opposite paleocurrent direction compared to the rest of the Sp_2 beds in the mosaic. This is overlain by medium beds of Sp_2 that mark reactivation surfaces, with an erosional base as the underlying dune migrated and is subsequently eroded by the migrating dune above it. After the deposition of a lenticular bed of facies He, higher energy conditions were re-established and medium-bedded Sp_2 is deposited over He, continuing dune migration until being mantled by more tabular bioturbated sandstones. This type of complexity is in stark contrast to the geometry of the same cross-stratified beds on the left side of the mosaic, which appear more tabular and laterally continuous (See Figure 9).

Locally the section records high flow which erodes and scours a tidal channel that is unrelated to dune migration (Figure 10). The channel is located in FA-1 at the base of the mosaic and consists of a concave-up base, overlain by mudstone deposited before cross-stratified sandstone subsequently infills the small channel and the bedform continues to migrate and thicken laterally. At the top of the mosaic a bed of cross-stratified sandstone of FA-1 displays a laterally migrating dune bedform showing a gradually reversing current direction.

7. Paleocurrents

The dip direction of foresets in the laterally continuous, planar cross-stratified sandstone (Sp_2) and, to a lesser extent, the conglomeratic, planar cross-stratified sandstone (Sp_3) yielded 165 paleocurrent measurements from all study sites (Figure 11). Those in Sp_2 display a bimodal distribution with a dominant west/west-northwest direction with a subordinate north/northeast direction. Locally, the dominant paleocurrent direction is to the southeast with a subordinate westerly direction. The presence of reactivation surfaces and rare bi-polar structures in the sets together with measured bimodal current directions infer a link with tidal action. Flow direction and paleogeography suggest sediment input broadly from the east, and the open ocean to the northwest.

Paleocurrent measurements for facies Sp_2 are oblique to the mapped faults near section B (see Figure 11), suggesting that the faults were not a controlling factor in shaping the local topography in the northern part of the study area.

Late early Cambrian syndepositional faulting is inferred by the changes in thickness of the clastic unit, as there are localities where the tan dolostone unit sits directly on Proterozoic basement but there is sandstone recorded on adjacent fault blocks. This relationship is observed near section A, as a north-east trending fault records no deposition of the clastic unit on the south-east side but section A occurs nearby on the north-west side of the fault. This is more likely to be a result of syndepositional faulting rather than simply gradual thinning onto an arch, though

gradual thinning does occur as well to the south towards section E. On the other hand, Section C exposes a linear scarp and karst surface developed on limestones of the Shaler Supergroup, which is onlapped by the clastic unit (Mathieu et al., 2013). The scarp was probably generated by faulting.

8. Discussion

8.1. Stratigraphic evolution

The unnamed clastic unit records late early Cambrian sedimentation on a passive margin and represents a major transgression onto the craton where marine sands mantled a low-relief topography. Complete Sections A and B show bioturbated sandstones (FA2) overlying cross-stratified sandstone sets (FA1) multiple times in the succession, with sharp contacts separating the facies associations (Figure 12). These contacts mark flooding surfaces where increased accommodation space allowed for renewed development of larger sandstone bodies and corresponding larger scale cross-stratification. Continued deposition filled declining growth of accommodation space with predominantly bioturbated sandstones until another flooding event created sufficient accommodation space for the next package of larger bedsets. The transition of FA2 into the oolitic ironstone (FA3) is gradational with the increase in content of hematite coatings around quartz sand. These coatings are localized into three thin horizons in Section B, two thin horizons in Section A, and a 3 m thick interval of thin beds at the top of the succession at Section D. The oolitic ironstone horizons mark periods of low sedimentation rates when iron became concentrated and calcite was the primary

cementing agent. The top of the clastic unit is retrogradational (FA4) and records a transition to open-shelf mudstones, which are themselves sharply overlain by carbonates of the tan dolostone unit. The tan dolostone unit is bioturbated and contains thrombolite patch reefs, indicating a shallow-marine platform setting. Its planar basal contact probably records a hiatus, and may be a regressive surface of marine erosion but if so it is unclear how much if any of the underlying mudstone has been removed. The regional extent of the tan dolostone unit marks a significant transgressive event during the early middle Cambrian and the carbonate platform persisted off and on until the Early Devonian.

Elsewhere on the island Section C consists of alternating intervals of FA1 and covered sections belonging to bioturbated sandstones of FA2 or FA3. Section D is composed of sandstone intervals of FA-2 and mudstone intervals of FA4, which are capped by ironstones of FA3. Section E is composed of interbedded sandstone and mudstone belonging to FA4. Sections A, B and C are 67 to 85 m thick and sandstones comprises greater than 90% of the succession. Section D is incomplete at 37 m but is composed of 75% sandstone, which is notably less than in the other sections. Thickness and proportion of sand decrease markedly in Section E, with only a few metres of mixed sandstone and mudstone deposited before the onset of carbonate deposition of the tan dolostone unit. The southward thinning and decrease in sand content (see Figure 3) parallels a thinning trend to the northeast where the tan dolostone unit also rests directly on Neoproterozoic rocks. These trends reflect the gently rising underlying topography over which transgression took place and

presumably reflect the location of the shoreline. Local paleotopographic highs are observed, where cross-stratified sandstones (Sp_2) rest directly on Proterozoic rocks despite the other side of the outcrop (100 m away) recording recessive sandstones overlying Proterozoic rocks. These variations in paleotopography reflect the undulating basement rock that the clastic unit mantles and directly affected the style of deposition at the Proterozoic - Paleozoic contact.

Section C is in close proximity to a major fault that runs a significant length across the island (the fault is located directly south of Section C in Figure 11). Paleocurrents of facies Sp_3 are mostly parallel to the fault trend, suggesting that faulting directly affected deposition in this area. The fault itself may have had considerable uplift, as no Cambrian sands are found to the southeast of it and Section E records very little sandstone interbedded with mudstone. Section A contains 85 m of sandstone and mudstone north-west of the north-east trending fault but nearby on the southeast side Cambrian dolostone rests on top of Neoproterozoic limestones, recording no deposition of the lower Cambrian clastic unit. This fault may have been a limiting factor in sandstone deposition and movement of the shoreline seems to have been largely fault-controlled in this area.

By contrast, facies Sp_1 and Sp_2 are deposited higher in the succession and are found all over the island. Further north from the major fault, Sp_1 and Sp_2 display different paleocurrent trends. Though the sections are bounded by faults, the paleocurrent data suggest that the grabens had little effect on current direction. Uplift

marginal to the grabens did not control movement of the shoreline, as mostly tabular geometry of underlying beds flattened the topography.

Much like the Cambrian basin of Northwest Territories, the basin on Victoria Island was bordered by positive elements during Cambrian time. Examples on Victoria Island where the tan dolostone unit sits directly on Neoproterozoic basement with sandstone recorded on adjacent fault blocks provides evidence that at least some of the arches and faults were active. The paleotopography of local subbasins and any tectonic warping would have created a coastline with bays and lagoons. Though faults and arches played a large role in subbasin shape in the northern mainland, their influence is notably less on Victoria Island. Maclean (2011) found that in the Mackenzie River valley of the northern mainland these elements were more subtle towards the northern part of the basin. This trend seems to have continued into Victoria Island.

8.2. Depositional model

The unnamed clastic unit was deposited in a shallow embayment that opened to the northwest, and the reworking of sandy sediment stored on the craton filled the undulating topography developed on the Neoproterozoic land surface. The presence of trace fossils low in the clastic unit indicates that there are no basal deposits of fluvial or backshore origin. Weathering of the nearby Franklin basalts and sills in an equatorial climate (e.g. Cocks and Torsvik, 2011) was protracted and substantial, leaving no trace of volcanic rock fragments. Iron concentration in a nearshore environmental setting during stillstands in sea level rise is consistent with other examples of Clinton ironstones

(e.g. Bayer, 1989; Young, 1992; Gross, 1995), despite uncertainties about the genesis and iron source of Phanerozoic ironstones (see Bekker et al., 2010, p. 491).

Embayment morphology can lead to strong tidal currents, tidal amplification and enhanced storm surges due to bathymetry and topographic constrictions as the rising water level inundates the irregular topography. These conditions give tidal deposits a higher chance of preservation than is the case elsewhere along the coast (Dalrymple, 2010). The largest tidal ranges occur within funnel-shaped embayments on passive continental margins (Archer and Hubbard, 2003).

Compound dune geometry in modern examples (e.g. Berné et al., 1993; Yoshida et al., 2004) record an upward increase in energy as indicated by the nature of the cross-stratification, typically recording bedsets of planar cross-stratified (=2D dunes) and trough cross-stratified (=3D dunes) sandstone (Dalrymple and Choi, 2007). However, the medium- to large-scale planar cross-stratification in the clastic unit reflects more or less uniform tidal current speeds in consistent water depths on a low-gradient seafloor and the transition from 2D to 3D dunes is not present here. The increase in energy is probably recorded by an upward energy increase from ripples into planar cross-stratification, though ripples were not often preserved.

Despite having a broad shape and lacking higher energy conditions the embayment appears to have had a macrotidal range (>4m) in a equatorial climate. This is attributed to larger astronomic tides as the Moon was closer to the Earth in Cambrian

time (Dalrymple, 2010). Following the environmental framework for tidal shelves of Desjardins et al. (2010a) the subtidal outer embayment sand dune complex is a bathymetric equivalent of the shoreface as commonly defined for wave-dominated settings (Plint, 2010) with the intertidal and supratidal environments lying landward of the shallow subtidal environment. No such facies are preserved, however, likely having been reworked during transgression before deposition of the tan dolostone unit.

The pattern of bioturbation in tidally influenced settings shows that the highest degree of bioturbation occurs where food resources are most abundant and overall sedimentation rates are low (i.e., bioturbation increases upwards from subtidal into intertidal settings) (Gingras et al., 2012). In shallow subtidal and shelf environments suspension feeders generally dominate in higher energy areas and the greatest trace-fossil diversity tends to occur in the mixed-flat area or, in the case of lower energy systems, in the sand flat (Mángano and Buatois, 2004; Buatois and Mángano, 2011). Ecological parameters in the subtidal region can also vary across a single sand body, which leads to localized colonization trends (Desjardins et al., 2012a). The ichnological diversity in the unnamed clastic unit is consistent with these trends, and dunes are, for the most part, non-bioturbated or contain just a few individual burrows belonging to *Skolithos*, representing the *Skolithos* ichnofacies. Moderate to high sedimentation rates and erosion resulting from continuous bedform migration are responsible for the lack of bioturbation. The sand flat exhibits a low-diversity *Cruziana* ichnofacies represented by trophic generalists, such as forms belonging to *Planolites*, *Palaeophycus* and *Teichichnus* plus the arthropod trace fossils *Rusophycus* isp. and *Cruziana* isp. This

trace fossil assemblage has been recognized in the outermost zones of marginal-marine depositional systems in Cambrian time, due in part to macroevolutionary controls on the trace makers (Buatois et al., 2005), although the lack of diminution in trace fossil size indicates dominantly marine conditions within the embayment. This ichnofauna shows preferential preservation in muddy sediment in low-energy conditions and more or less continuous colonization windows.

9. Conclusions

This contribution presents a sedimentological analysis of the hitherto unstudied, informally named lower Cambrian clastic unit at the base of the Paleozoic section in western Victoria Island, Canadian Arctic Islands. Sandstones exposed around the head of Minto Inlet record deposition in a tide-dominated embayment on the passive margin of Laurentia. The basin opened to the northwest, and stratigraphic thinning towards both the south and northeast shows the direction of the paleoshoreline. Paleocurrent measurements and thickness variation suggest that deposition was affected by undulating topography on the Proterozoic basement, as well as by syndepositional faulting in some parts of the basin. Four facies associations represent outer embayment sand-dune complex, inner embayment sand flat, coastal lagoon, and offshore muddy shelf. Bioturbation in the form of a typical early Cambrian suite of shallow-subtidal ichnofossils predominated in the inner embayment and coastal lagoon settings, and iron enrichment characterizes several levels in the coastal lagoon. The mostly tabular, sheet-like geometry of the sandstones is attributed to sediment deposition under essentially uniform current speeds at consistent water depths in a low-gradient setting.

Approximately shoreline orthogonal paleocurrents are considered indicative of a tidal origin of these currents. The largest cross-stratified dunes are in the middle part of the succession in outcrops located in the outermost part of the embayment, and these are taken as evidence for migration under elevated tidal currents in this zone. The absence of hummocky cross-stratification argues against the influence of major storms in this region.

References

Aitken, J.D., 1993. Cambrian and Lower Ordovician – Sauk Sequence. Subchapter 4B. In: Stott, D.F., Aitken, J.D. (Eds.), Sedimentary Cover of the Craton in Canada. Geological Survey of Canada, Geology of Canada, no. 5, pp. 96–124.

Aitken, J. D., 1997. Stratigraphy of the Middle Cambrian Platformal Succession, Southern Rocky Mountains. Geological Survey of Canada Bulletin 398, 322 pp.

Aitken, J.D., Macqueen, R.W., Usher, J.L., 1973. Reconnaissance studies of Proterozoic and Cambrian stratigraphy, lower Mackenzie River area (Operation Norman), District of Mackenzie. Geological Survey of Canada Paper 73-9, 178 pp.

Allen, J.R.L., 1980. Sand waves: a model of origin and internal structure. Sedimentary Geology 26, 281–328.

Archer, A.W., Hubbard, M.S., 2003. Highest tides of the world. In: Chan, M.A., Archer, A.W. (Eds.), Extreme Depositional Environments: Mega End Members in Geologic Time. Geological Society of America, Special Paper 370, pp. 151–173.

Ashley, G.M., 1990. Classification of large-scale subaqueous bedforms: a new look at an old problem. Journal of Sedimentary Petrology 60, 160–172.

Bayer, U., 1989. Stratigraphic and enviromental patterns of ironstone deposits. In: Young, T.P., Taylor, W.E.G. (Eds.), Phanerozoic Ironstones. Geological Society of London, Special Publication 46, pp. 105–117.

Bekker, A., Slack, J.F., Planavsky, N., Krapež, B., Hofmann, A., Konhauser, K.O., Rouxel, O.J., 2010. Iron formation: The sedimentary product of a complex interplay among mantle, tectonic, oceanic, and biospheric processes. Economic Geology 105, pp. 467–508.

Berné, S., Castaing, P., Le Drezen, E., Lericolais, G., 1993. Morphology, internal structure, and reversal of asymmetry of large subtidal dunes in the entrance to the Gironde Estuary (France). Journal of Sedimentary Petrology 63, 780–793.

Bond, G.C., Nickerson, P.A., Kominz, M.A., 1984. Breakup of a supercontinent between 625 Ma and 555 Ma: new evidence and implications for continental histories. Earth and Planetary Science Letters 70, 325–345.

Bédard, J.H., Naslund, H. R., Nabelek, P., Winpenny, A., Hryciuk, M., Macdonald, W., Hayes, B., Steigerwaldt, K., Hadlari, T., Rainbird, R., Dewing, K., Girard, É., 2012. Fault-mediated melt ascent in a Neoproterozoic continental flood basalt province, the Franklin sills, Victoria Island, Canada. Geological Society of America Bulletin 124, 723–736.

Buatois, L.A., Mángano, M.G., 2011. Ichnology: Organism-Substrate Interactions in Space and Time. Cambridge University Press, Cambridge, 358 pp.

Buatois, L.A., Gingras, M.K., MacEachern, J.D., Mángano, M.G., Zonneveld, J.P., Pemberton, S.G., Netto, R.G., Martin, A., 2005. Colonization of Brackish-Water Systems through Time: Evidence from the Trace-Fossil Record. Palaios 20, 321–347.

Cant, D.J., Hein, F.J., 1986. Depositional sequences in ancient shelf sediments: some contrasts in style. In: Knight, R.J., McLean, J.R. (Eds), Shelf Sands and Sandstones. Canadian Society of Petroleum Geologists Memoir 11, pp. 303–312.

Cawood, P.A., Nemchin, A.A., Strachan, R., Prave, T., Krabbendam, M., 2007. Sedimentary basin and detrital zircon record along East Laurentia and Baltica during assembly and breakup of Rodinia. Journal of the Geological Society of London 164, 257–275.

Chafetz, H.S., Meredith, J.C., Kocurek, G., 1986. The Cambro-Ordovician Bliss Formation, southwestern New Mexico, U.S.A. – Progradational sequences on a mixed siliciclastic and carbonate shelf. Sedimentary Geology 49, 201–221.

Cocks, L.R.M., Torsvik, T.H., 2011. The Palaeozoic geography of Laurentia and western Laurussia: a stable craton with mobile margins. Earth-Science Reviews 106, 1–51.

Cook, D.G., MacLean, B.C., 2004. Subsurface Proterozoic stratigraphy and tectonics of the western plains of the Northwest Territories. Geological Survey of Canada Bulletin 575, 1 CD, 91 pp.

Cotter, E., Link, J.E., 1993. Deposition and diagenesis of Clinton ironstones (Silurian) in the Appalachian Foreland Basin of Pennsylvania. Geological Society of America Bulletin 105, 911–922.

Dalrymple, R.W., 1984. Morphology and internal structure of sandwaves in the Bay of Fundy. Sedimentology 31, 365–382.

Dalrymple, R.W., 2010. Tidal Depositional Systems. In: James, N.P., Dalrymple, R.W. (Eds.), Facies Models 4. Geological Association of Canada, St. John's, Geotext 6, pp. 201–231.

Dalrymple, R.W., Choi, K., 2007. Morphologic and facies trends through the fluvial–marine transition in tide-dominated depositional systems: a schematic framework for environmental and sequence stratigraphic interpretation. Earth-Science Reviews 81, 135–174.

Dalrymple, R.W., Rhodes, R.N., 1995. Estuarine dunes and bars. In: Perillo, G.M.E. (Ed), Geomorphology and Sedimentology of Estuaries. Elsevier, Amsterdam, pp. 359–422.

Dalrymple, R.W., Narbonne, G.M., Smith, L., 1985. Eolian action in the distribution of Cambrian shales in North America. Geology 13, 607–610.

Davidson, A., 2008. Late Paleoproterozoic to mid-Neoproterozoic history of northern Laurentia: An overview of central Rodinia. Precambrian Research 160, 5–22.

Denyszyn, S.W., Halls, H.C., Davis, D.W., 2006. A paleomagnetic, geochemical and U-Pb geochronological comparison of the Thule (Greenland) and Devon Island (Canada) dyke swarms and its relevance to the Nares Strait problem. Polarforschung 74, 63–75.

Desjardins, P.R., Buatois, L.A., Pratt, B.R., Mángano, M.G., 2012a. Sedimentological–ichnological model for tide-dominated shelf sandbodies: Lower Cambrian Gog Group of western Canada. Sedimentology 59, 1452–1477.

Desjardins, P.R., Buatois, L.A., Pratt, B.R., Mángano, M.G., 2012b. Forced regressive tidal flats: response to falling sea level in tide-dominated settings. Journal of Sedimentary Research 82, 149–162.

Desjardins, P.R., Mángano, M.G., Buatois, L.A., Pratt, B.R., 2010b. *Skolithos* pipe rock and associated ichnofabrics from the southern Rocky Mountains, Canada: colonisation trends and environmental controls in an Early Cambrian sand-sheet complex. Lethaia 43, 507–528.

Desjardins, P.R., Pratt, B.R., Buatois, L.A., Mángano, M.G., 2010a. Stratigraphy and sedimentary environments of the Lower Cambrian Gog Group in the southern Rocky Mountains of western Canada: evolution of transgressive sandstones on a broad continental margin. Bulletin of Canadian Petroleum Geology 58, 1–37.

Dewing, K., Nowlan, G., 2012. The Lower Cambrian to Lower Ordovician carbonate platform and shelf margin, Canadian Arctic Islands. In: Derby, J. R., Fritz, R. D., Longacre, S. A., Morgan, W. A., Sternbach, C. A. (Eds.), The great American carbonate bank: The geology and economic resources of the Cambrian – Ordovician Sauk megasequence of Laurentia. American Association of Petroleum Geologists Memoir 98, pp. 627–647.

Dewing, K., Harrison, J.C., Pratt, B.R., Mayr, U., 2004. A probable late Neoproterozoic age for the Kennedy Channel and Ella Bay formations, northeastern Ellesmere Island, and its implications for a passive margin history of the Canadian Arctic. Canadian Journal of Earth Sciences 41, 1013–1025.

Dewing, K., Mayr, U., Harrison, J.C., de Freitas, T., 2008. Upper Neoproterozoic to Lower Devonian stratigraphy of northeast Ellesmere Island. In: Mayr, U. (Ed.), Geology of Northeast Ellesmere Island Adjacent to Kane Basin and Kennedy Channel, Nunavut. Geological Survey of Canada Bulletin 592, pp. 31–108.

Dewing, K., Pratt, B.R., Hadlari, T., Brent, T., Bédard, J., Rainbird, R.H., 2013. Newly identified “Tunnunik” impact structure, Prince Albert Peninsula, northwestern Victoria Island, Arctic Canada. Meteoritics & Planetary Science 48, 211–223.

Dilliard, K.A., Pope, M.C., Coniglio, M., Hasiotis, S.T., Lieberman, B.S., 2010. Active synsedimentary tectonism on a mixed carbonate–siliciclastic continental margin: third-order sequence stratigraphy of a ramp to basin transition, lower Sekwi Formation, Selwyn Basin, Northwest Territories, Canada. Sedimentology 57, 513–542.

Dixon, J., Stasiuk, L.D., 1998. Stratigraphy and hydrocarbon potential of Cambrian strata, northern Interior Plains, Northwest Territories. Bulletin of Canadian Petroleum Geology 46, 445–470.

Driese, S.G., Byers, C.W., Dott, R.H., 1980. Tidal deposition in the basal Upper Cambrian Mt. Simon Formation in Wisconsin. Journal of Sedimentary Petrology 51, 367–381.

Fritz, W.H., 1972. Lower Cambrian trilobites from the Sekwi Formation type section, Mackenzie Mountains, northwestern Canada. Geological Survey of Canada Bulletin 212, 90 pp.

Fritz, W.H., 1973. Medial Lower Cambrian trilobites from the Mackenzie Mountains, northwestern Canada. Department of Energy, Mines and Resources, Geological Survey of Canada Paper 73–24, 43 pp.

Gingras, M.K., Pemberton, S.G., Saunders, T., Clifton, H.E., 1999. The ichnology of modern and Pleistocene brackish-water deposits at Willapa Bay, Washington: variability in estuarine settings. Palaios 14, 352–374.

Gingras, M.K., MacEachern, J.D., Dashtgard, S.E., 2012. The potential of trace fossils as tidal indicators in bays and estuaries. Sedimentary Geology 279, 97–106.

Gross, G.A., 1995. Stratiform Iron. In: Eckstrand, O.R., Sinclair, W.D., Thorpe, R.I. (Eds.), Geology of Canadian Mineral Deposit types. Geological Survey of Canada Series no. 8, pp. 41–80.

Hadlari, T., 2013. Reconstructing the Neoproterozoic-lower Paleozoic Franklinian Margin of the Northwestern Canadian Arctic. Polar Petroleum Potential Conference & Exhibition, Stavanger, Norway.

Hadlari, T., Davis, W.J., Dewing, K., Heaman, L.M., Lemieux, Y., Ootes, L., Pratt, B.R., Pyle, L.J., 2012. Two detrital zircon signatures for the Cambrian passive margin of northern Laurentia highlighted by new U-Pb results from northern Canada. Geological Society of America Bulletin 124, 1155–1168.

Harlan, S.S., Heaman, L., LeCheminant, A.N., Premo, W.R., 2003. Gunbarrel mafic magmatic event: A key 780 Ma time marker for Rodinia plate reconstructions. Geology 31, 1053–1056.

Harrison, J.C., 1995. Melville Island's salt-based fold belt, Arctic Canada. Geological Survey of Canada Bulletin 472, 331 pp.

Heaman, L.M., LeCheminant, A.N., Rainbird, R.H., 1992. Nature and timing of Franklin igneous events, Canada: Implications for a Late Proterozoic mantle plume and the break-up of Laurentia. Earth and Planetary Science Letters 109, 117–131.

Hoffman, P.F., 1988. United plates of America, the birth of a craton: Early Proterozoic assembly and growth of Laurentia. Annual Review of Earth and Planetary Sciences 16, 543–603.

Ineson, J.R., Peel, J.S., 1997. Cambrian shelf stratigraphy of North Greenland. Geology of Greenland Survey Bulletin 173, 120 p.

Ineson, J.R., Peel, J.S., 2011. Geological and depositional setting of the Sirius Passet Lagerstätte (Early Cambrian), North Greenland. Canadian Journal of Earth Sciences 48, 1259–1281.

Johnson, H.D., B.K. Levell, 1995. Sedimentology of a transgressive, estuarine sand complex: The Lower Cretaceous Woburn Sands (Lower Greensand), southern England. In: A.G. Plint (Ed.), Sedimentary Facies Analysis; a Tribute to the Research and Teaching of Harold G. Reading. International Association of Sedimentologists Special Publication 22, pp. 17–46.

Kearsley, A.T., 1989. Iron-rich ooids, their mineralogy and microfabric: clues to their origin and evolution. In: Young, T.P., Taylor, W.E.G. (Eds.), Phanerozoic Ironstones. Geological Society of London Special Publication 46, pp. 141–164.

Kimberley, M.M., 1994. Debate about ironstone – has solute supply been surficial weathering, hydrothermal convection, or exhalation of deep fluids. Terra Nova 6, 116–132.

Kimmig, J., Pratt, B.R., in press. Soft-bodied biota from the Middle Cambrian (Drumian) Rockslide Formation, Mackenzie Mountains, northwestern Canada. Journal of Paleontology.

Levy, M., Christie-Blick, N., 1991. Tectonic subsidence of the early Paleozoic passive continental margin in eastern California and southern Nevada. Geological Society of America Bulletin 103, 1590–1606.

Lickorish, W.H., Simony, P.S., 1995. Evidence for late rifting of the Cordilleran margin outlined by stratigraphic division of the Lower Cambrian Gog Group, Rocky Mountain Main Ranges, British Columbia and Alberta. Canadian Journal of Earth Sciences 32, 860–874.

Lochman-Balk, C., 1971. The Cambrian of the craton of the United States. In: Holland, C.H. (Ed.), Cambrian of the New World. London, Wiley-Interscience, pp. 79–167.

Long, D.G.F., Yip, S.S., 2009. The Early Cambrian Bradore Formation of southeastern Labrador and adjacent parts of Quebec: architecture and genesis of clastic strata on an early Paleozoic wave-swept shallow marine shelf. Sedimentary Geology 215, 50–69.

MacEachern, J.A., Bann, K.L., 2008. The role of ichnology in refining shallow marine facies models. In: Hampson, G.J., Steel, R.J., Burgess, P.M., Dalrymple, R.W. (Eds.), Recent Advances in Models of Siliciclastic Shallow-Marine Stratigraphy. Society for Sedimentary Geology Special Publication 90, pp. 73–116.

MacEachern, J.A., Gingras, M.K., 2007. Recognition of brackish-water trace fossil suites in the Cretaceous Western Interior Seaway of Alberta, Canada. In: Bromley, R.G., Buatois, L.A., Mángano, G., Genise, J.F., Melchor, R.N. (Eds.), Sediment-Organism Interactions: A Multifaceted Ichnology. Society for Sedimentary Geology Special Publication 88, pp. 149–193.

Maclean, B.C., 2011. Tectonic and stratigraphic evolution of the Cambrian basin of northern Northwest Territories. Bulletin of Canadian Petroleum Geology 59, 172–194.

MacNaughton, R.B., Dalrymple, R.W., Narbonne, G.M., 1997. Early Cambrian braid-delta deposits, Mackenzie Mountains, north-western Canada. Sedimentology 44, 587–609.

MacNaughton, R.B., Narbonne, G.M., Dalrymple, R.W., 2000. Neoproterozoic slope deposits, Mackenzie Mountains, northwestern Canada: Implications for passive-margin development and Ediacaran faunal ecology. Canadian Journal of Earth Sciences 37, 997–1020.

MacNaughton, R.B., Pratt, B.R., Fallas, K.M., 2013. Observations on Cambrian stratigraphy in the eastern Mackenzie Mountains, Northwest Territories. Geological Survey of Canada, Current Research 2013–10, 7 pp.

Mángano, M.G., Buatois, L.A., 2004. Reconstructing Early Phanerozoic intertidal ecosystems: Ichnology of the Cambrian Campanario Formation in northwest Argentina. In: Webby, M.D., Mángano, M.G., Buatois, L.A. (Eds.), Trace Fossils in Evolutionary Palaeoecology. Fossils and Strata 51, pp. 17–38.

Mathieu, J., Turner, E.C., Rainbird, R.H., 2013. Sedimentary architecture of a deeply karsted Precambrian-Cambrian unconformity, Victoria Island, Northwest Territories. Geological Survey of Canada, Current Research 2013–1, 15 pp.

Maynard, J.B., Van-Houten, F.B., 1992. Descriptive model of oolitic ironstones. U.S. Geological Survey Bulletin 2004, pp. 39−40.

McKie, T., 1990. Tidal and storm influenced sedimentation from a Cambrian transgressive passive margin sequence. Journal of the Geological Society of London 147, 785–794.

Nio, S.D., Yang, C.S., 1991. Diagnostic attributes of clastic tidal deposits: a review. In: Smith, D.G., Reinson, G.E., Zaitlin, B.A., Rahmani, R.A. (Eds.), Clastic Tidal Sedimentology. Canadian Society of Petroleum Geologists Memoir 16, pp. 3–28.

Pearson, N.J., Mángano, M.G., Buatois, L.A., Casadío, S., Raising, M.R., 2013. Environmental variability of *Macaronichnus* ichnofabrics in Eocene tidal-embayment deposits of southern Patagonia, Argentina. Lethaia 46, 341–354.

Peel, J.S., Dawes, P.R., Collinson, J.D., Christie, R.L., 1982. Proterozoic-basal Cambrian stratigraphy across Nares Strait; correlation between Inglefield Land and Bache Peninsula. In: Dawes, P.R., Kerr, J. W. (Eds.), Nares Strait and the Drift of Greenland; A Conflict in Plate Tectonics, Meddelelserom Grønland, Geoscience 8, pp. 105–115.

Pemberton, S.G., Frey, R.W., Ranger, M.J., MacEachern, J.A., 1992. The conceptual framework of ichnology. In: Pemberton, S.G. (Ed), Applications of ichnology to petroleum exploration. Society for Sedimentary Geology Core Workshop 17, pp. 1– 32.

Plint, A.G., 2010. Wave- and storm-dominated shoreline and shallow-marine systems. In: James, N.P., Dalrymple, R.W. (Eds.), Facies Models 4. Geological Association of Canada, St. John's, Geotext 6, pp. 167–200.

Pollard, J.E., Goldring, R., Buck, S.G., 1993. Ichnofabrics containing *Ophiomorpha*: significance in shallow-water facies interpretation. Journal of the Geological Society of London 150, 149–164.

Pratt, B.R., 2002. Tepees in peritidal carbonates; origin via earthquake-induced deformation, with example from the Middle Cambrian of Western Canada. Sedimentary Geology 153, 57–64.

Prave, A.R., 1991. Depositional and sequence stratigraphic framework of the Lower Cambrian Zabriskie Quartzite: implications for regional correlations and the Early Cambrian paleogeography of the Death Valley region of California and Nevada. Geological Society of America Bulletin 104, 505–515.

Rainbird, R.H., 1993. The sedimentary record of mantle plume uplift preceding eruption of the Neoproterozoic Natkusiak flood basalt. Journal of Geology 101, 305–318.

Rainbird, R.H., LeCheminant, A.N., Lawyer, J.I., 1996. The Duke of York and related Neoproterozoic inliers of southern Victoria Island, District of Franklin, Northwest Territories. In: Current Research: Geological Survey of Canada Paper 1996-E, pp. 125–134.

Rainbird, R. H., Davis, W. J., Pehrsson, S. J., Wodicka, N., Rayner, N., Skulski, T., 2010. Early Paleoproterozoic supracrustal assemblages of the Rae domain, Nunavut, Canada: intracratonic basin development during supercontinent break-up and assembly. Precambrian Research 181, 167–186.

Rainbird, R.H., McNicoll, V.J., Thériault, R.J., Heaman, L.M., Abbott, J.G., Long, D.G.F., Thorkelson, D.J., 1997. Pan-continental river system draining Grenville Orogen recorded by U-Pb and Sm-Nd geochronology of Neoproterozoic quartzarenites and mudrocks, northwestern Canada. Journal of Geology 105, 1–17.

Rainbird, R.H., Stern, R.A., Khudoley, A.K., Kropachev, A.P., Heaman, L.M., Sukhorukov, V.I., 1998. U-Pb geochronology of Riphean sandstone and gabbro from southeast Siberia and its bearing on the Laurentia–Siberia connection. Earth and Planetary Science Letters 164, 409–420.

Ross, G.M., 1991. Tectonic setting of the Windermere Supergroup revisited. Geology 19, 1125–1128.

Runkel, A.C., Miller, J.F., McKay, R.M., Palmer, A.R., Taylor, J.F., 2008. The record of time in cratonic interior strata: does exceptionally slow subsidence necessarily result in exceptionally poor stratigraphic completeness? In: Pratt, B.R., Holmden, C. (Eds.), Dynamics of Epeiric Seas. Geological Association of Canada, Special Paper No. 48, pp. 341–362.

Sanford, B.V., Arnott, R.W.C., 2009. Stratigraphic and structural framework of the Potsdam Group in eastern Ontario, western Quebec, and northern New York State. Geological Survey of Canada Bulletin 597, 83 pp.

Simpson, E.L., Eriksson, K.A., 1990. Early Cambrian progradational and transgressive sedimentation patterns in Virginia: an example of the early history of a passive margin. Journal of Sedimentary Petrology 60, 84–100.

Simpson, E.L., Dilliard, K.A., Rowell, B.F., Higgins, D., 2002. The fluvial to marine transition within the post-rift Lower Cambrian Hardyston Formation, eastern Pennsylvania, USA. Sedimentary Geology 147, 127–142.

Sixsmith, P.J., Hampson, G.J., Gupta, S., Johnson, H.D., Fofana, J.F., 2008. Facies architecture of a net transgressive sandstone reservoir analog: the Cretaceous Hosta Tongue, New Mexico. American Association of Petroleum Geologists Bulletin 92, 513–547.

Taylor, A., Goldring, R.,1993. Description and analysis of bioturbation and ichnofabric. Journal of the Geological Society of London 150, 141–148.

Teyssen, T.A.L., 1984. Sedimentology of the Minette oolitic ironstones of Luxembourg and Lorraine: a Jurassic subtidal sandwave complex. Sedimentology 31, 195–211.

Thomson, D., Rainbird, R.H., Dix, G., 2014. Architecture of a Neoproterozoic intracratonic carbonate ramp succession: Wynniatt Formation, Amundsen Basin, Arctic Canada. Sedimentary Geology 299, 119–138.

Thorsteinsson, R., Tozer, E.T., 1962. Banks, Victoria and Stefansson Islands, Arctic Archipelago. Geological Survey of Canada Memoir 330, 85 pp.

Trettin, H.P., 1991. Tectonic framework. In: Trettin, H.P. (Ed.), Geology of the Innuitian Orogen and Arctic Platform of Canada and Greenland. Geological Survey of Canada, Geology of Canada 3, pp. 59–66.

Turner, E.C., Roots, C.F., MacNaughton, R.B., Long, D.F.G., Fischer, B.F., Gordey, S.P., Martel, E., Pope, M.C., 2011. Stratigraphy. In: Martel, E., Turner, E.C., Fischer, B.J. (Eds.), Geology of the central Mackenzie Mountains of the northern Canadian Cordillera, Sekwi Mountain (105P), Mount Eduni (106A), and northwestern Wrigley Lake (95M) map-areas, Northwest Territories. NWT Special Volume 1, NWT Geoscience Office, pp. 31–192.

Van Houten, F., 2000. Ooidal ironstones and phosphorites – a comparison from a stratigrapher's view. In: Glenn, C.R., Prévôt-Lucas, L., Lucas, J. (Eds.), Marine authigenesis: from global to microbial. Society for Sedimentary Geology Special Publication 66, pp. 127–132.

Yoshida, S., Johnson, H.D., Pye, K., Dixon, R.J., 2004. Transgressive changes from tidal estuarine to marine embayment depositional systems: the Lower Cretaceous Woburn Sands of southern England and comparison with Holocene analogs. American Association of Petroleum Geologists Bulletin 88, 1433–1460.

Young, T.P., 1989. Phanerozoic Ironstones: an introduction and review. In: Young, T.P., Taylor, W.E.G. (Eds.), Phanerozoic Ironstones. Geological Society of London, Special Publication 46, pp. ix–xxv.

Young, T.P., 1992. Ooidal ironstones from Ordovician Gondwana: a review. Palaeogeography, Palaeoclimatology, Palaeoecology 99, 321–347.

LIST OF TABLE AND FIGURE CAPTIONS

Figure 1: Geology of the Minto Inlier (modified from Dewing et al., 2013).

Figure 2: Correlation chart of lower Cambrian formations in present-day northern Laurentia. The chronostratigraphic subdivisions are the current global series, North American stages, and the traditional genus-based trilobite biozones for the Laurentian early Cambrian. Stratigraphy for the Mackenzie Mountains is taken from Turner et al. (2011). That for the northern Interior Plains of the Mackenzie River valley region is taken from MacNaughton et al. (2013). The nomenclature for western Victoria Island is currently informal (Dewing et al., 2013); the ages of the formations are from trilobite collections under study by BRP. The stratigraphy of Inglefield Land of northwestern Greenland is also applicable to Bache Peninsula of central-eastern Ellesmere Island (Peel et al., 1982). The stratigraphy of northern Ellesmere Island is taken from Dewing et al. (2008). The exact ages of the unnamed, Ritter Bay and Rawlings Bay formations are unknown. That of North Greenland is from Ineson and Peel (1997, 2011). The Portfjeld Formation of North Greenland is considered equivalent to the Ella Bay Formation but may be as young as earliest Cambrian. Ages of the base of the transgressive sandstones comprising the Mount Clark and Dallas Bugt formations, as well as the “Clastic unit” are uncertain. These are the most in-board regions.

Table 1: Facies in the unnamed clastic unit, Victoria Island.

Table 2: Location of measured sections and drill core.

Figure 3: Stratigraphic cross-section of sections A-E. The overlying tan dolostone unit is used as a datum.

Figure 4: Planar cross-laminated structures in the unnamed clastic unit, Victoria Island. A. Stacked beds of cross-stratified sandstone (Sp_2) with opposing foreset directions overlying recessive bioturbated sandstones (S_{B1} - S_{B2}). B. Plan-view of de-watering structure in conglomeritic planar cross-laminated sandstone (Sp_3). Scale bar is 7 cm. C. Block of cross-laminated sandstone (Sp_2). Upper portion contains cross-lamination with a rounded, convex upward foreset top and reactivation surface. Knife at top is 9 cm. D. Cross-sectional view of conglomeritic planar cross-laminated sandstone (Sp_3). Knife at top right is 9 cm. E. Foresets of planar cross-laminated sandstone (Sp_1). Middle set contains a reactivation surface and rounded, convex-upward foreset top. Knife is 9 cm. F. Planar cross-laminated sandstone (Sp_2) with ripple-top overlying interbedded mudstone and sandstone (He). Camera lens is 7 cm.

Figure 5: Large bedded planar cross-laminated sandstone (Sp_2). A. Stacked beds of large bedded planar cross-laminated sandstone. Person is 1.7 m. B. Planar cross-laminated sandstone with coarse sand in the foresets. Hammer is 30 cm. C. Scour surface separating two large bedded planar cross-laminated sandstones. D. Smaller set of planar cross-laminated sandstone migrating over large bedded sets. Person is 1.7 m.

Figure 6: Facies in the unnamed clastic unit, Victoria Island. A. Massive sandstone (Sm) overlying Proterozoic dolostone. Person is 1.8 m. B. Wave-rippled sandstone (Sw) overlying recessive bioturbated sandstone (S_{B1}). Pen is 15 cm. C. Thinly interbedded mudstone and sandstone (He) separating planar cross-laminated sandstone (Sp_2). Knife is 9 cm. D. Plane-laminated sandstone (S_L) with *Diplocraterion* isp. and ?*Arenicolites* isp.. E. Recessive bioturbated sandstone (S_{B1}) with *Skolithos* isp.. F. Oolitic ironstone horizon in between beds of bioturbated sandstone (S_{B1} and S_{B2}).

Figure 7: Ichnofossils preserved on bed soles (with positive hyporelief) in facies S_{B1}, S_{B2} and He. All but E are in plan view. Scale bars are 2 cm. ASM = arthropod scratch marks. A. *Phycodes* isp., *Skolithos* isp. and ASM (S_{B2}). B. *Rusophycus* isp., *Palaeophycus* isp., *Skolithos* isp. and ASM (S_{B1}). C. *Skolithos* isp., *Palaeophycus* isp., ?*Teichichnus* isp. and ASM in plan-view (S_{B2}). D. *Rusophycus jenningsi* (He). E. Lateral view of *Rusophycus jenningsi* shown in D. F. *Palaeophycus* isp. and ?*Helminthopsis* isp. (S_{B2}).

Figure 8: Thin section of oolitic ironstone in facies S_O. A, B. Sub-rounded to well-rounded quartz grains with echinoderm ossicles and phosphatic brachiopod valve fragments with blocky calcite cement. All fragments and grains are coated in hematite. Plane polarized light. Section D, + 37 m.

Figure 9: Photomosaic of east-facing cliff at section B. A. Original photomosaic. The water level is located at +42 m in the measured section shown in Figures 3 and 12. B.

Tracing of selected bedding surfaces and stratigraphic position of facies associations. Lowest exposed interval consists of bioturbated sandstones of FA-2 and exhibits mostly tabular bedding. Overlying FA-1 exhibits tabular and gently undulating to lenticular bedding, with lenticular geometries at the right side. Dip directions of cross-lamination where visible are shown by oblique lines. The overlying FA-2 and ironstone-bearing FA-3 are tabular-bedded. i = ironstone horizon. The top of the section consists of a thin interval of FA-2 overlain by recessive mudstones comprising FA-4. Facies association contacts are marked by arrows.

Figure 10: Photomosaic of south-facing cliff at section B. Right side is about 30 m away from the right side of photomosaic in Figure 9 and approximately at right angles to it. A. Original photomosaic. The base of the cliff is 7 m below the lowest sandstone interval in Figure 9 and begins at +35 m in the measured section shown in Figures 3 and 12. B. Tracing of selected bedding surfaces and stratigraphic position of facies associations. Lowest exposed interval consist of tabular and undulating beds of FA-1, including a marked scour surface. The overlying FA-2 exhibits mostly tabular bedding. The highest interval consists of FA-1 and shows tabular and gently undulating to lenticular bedding geometries. Dip directions of cross-lamination where visible are shown by oblique lines. Facies association contacts are marked by arrows.

Figure 11: Paleocurrent data and geology of the Minto Inlier (modified from Dewing et al., 2013). Paleocurrent measurements are from cross-lamination in facies Sp_2 and Sp_3.

Figure 12: Facies association distribution in Section A and B (legend is in Figure 3).

FIGURES

Figure 1:

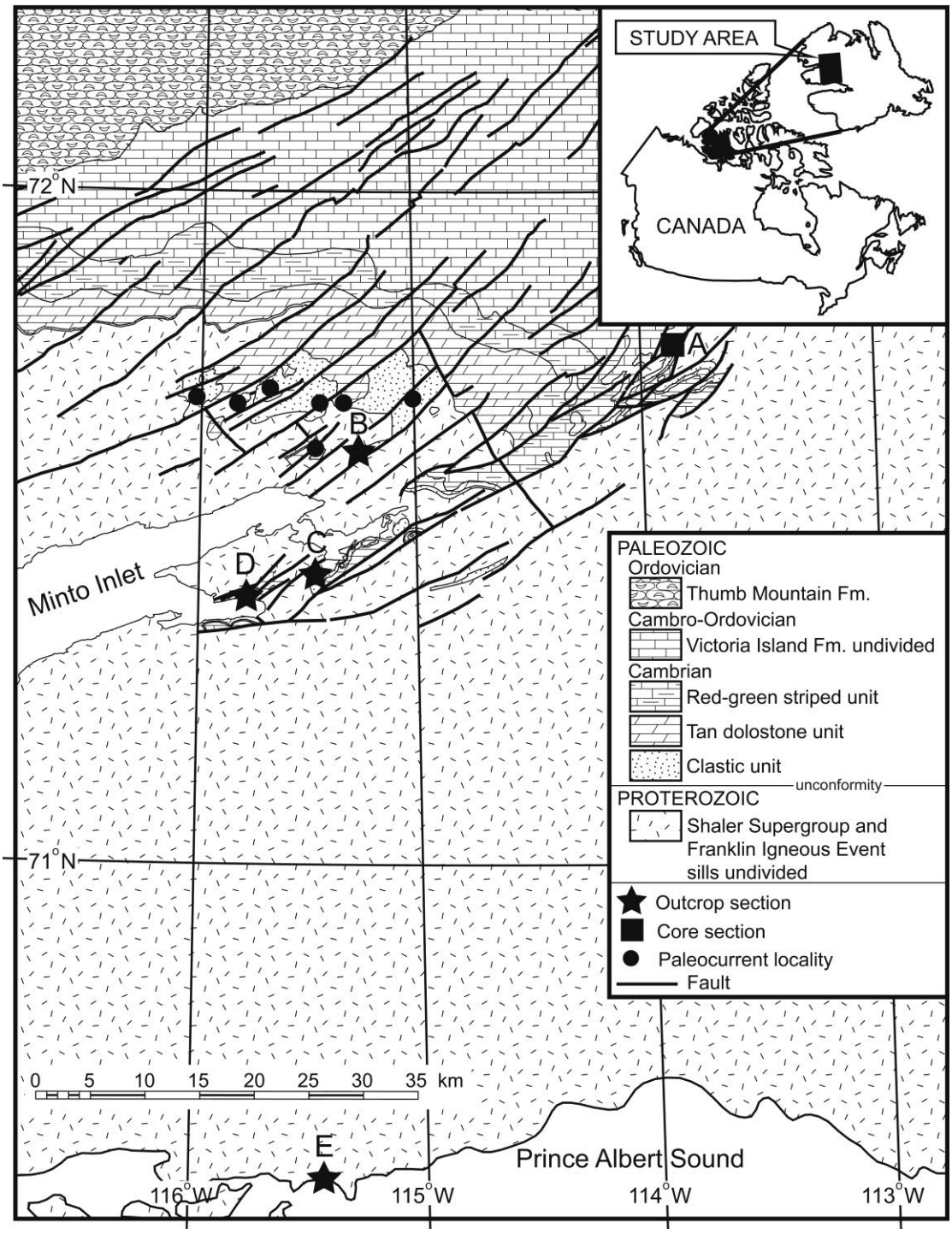

Figure 2:

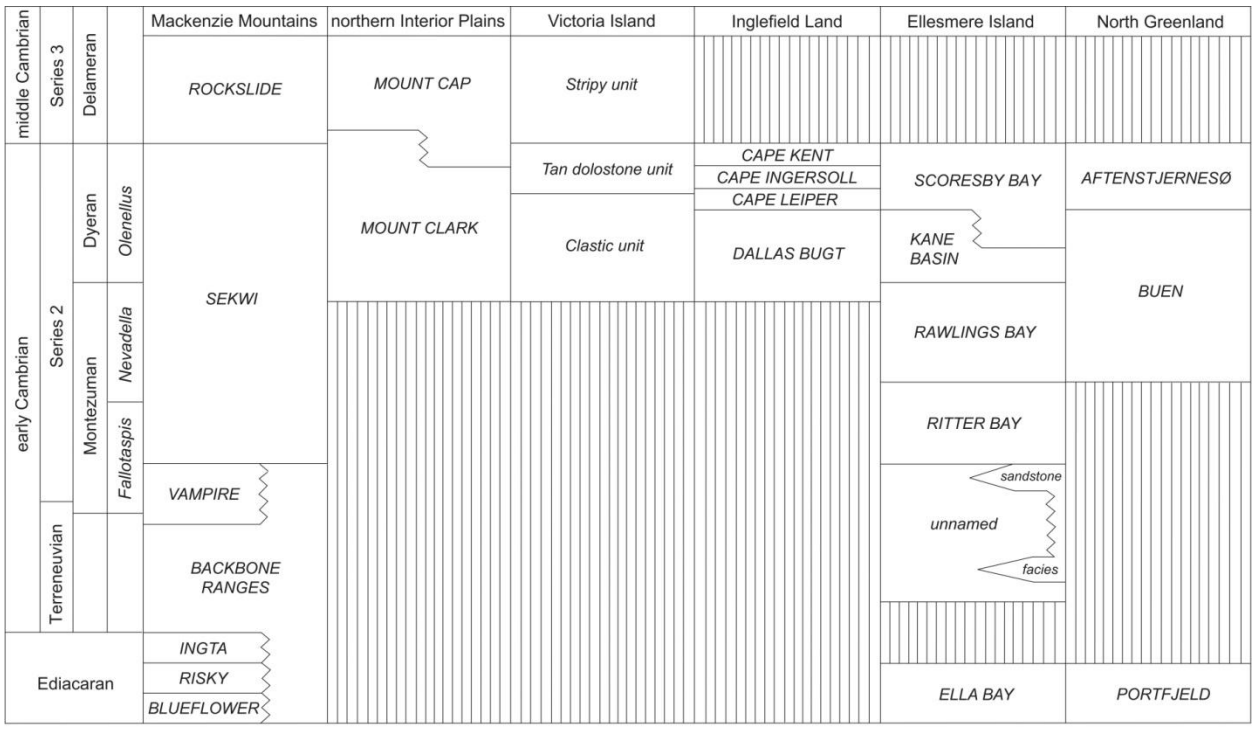
middle Cambrian
Series 3
Delamerian
early Cambrian
Series 2
Dyeran
Olenellus
Montezuman
Nevadella
Fallotaspis
Terreneuvian
Ediacaran
Mackenzie Mountains
ROCKSLIDE
SEKWI
VAMPIRE
BACKBONE RANGES
INGTA
RISKY
BLUEFLOWER
northern Interior Plains
MOUNT CAP
MOUNT CLARK
Victoria Island
Stripy unit
Tan dolostone unit
Clastic unit
Inglefield Land
CAPE KENT
CAPE INGERSOLL
CAPE LEIPER
DALLAS BUGT
Ellesmere Island
SCORESBY BAY
KANE BASIN
RAWLINGS BAY
RITTER BAY
sandstone
unnamed
facies
ELLA BAY
North Greenland
AFTENSTJERNESØ
BUEN
PORTFJELD

Figure 3

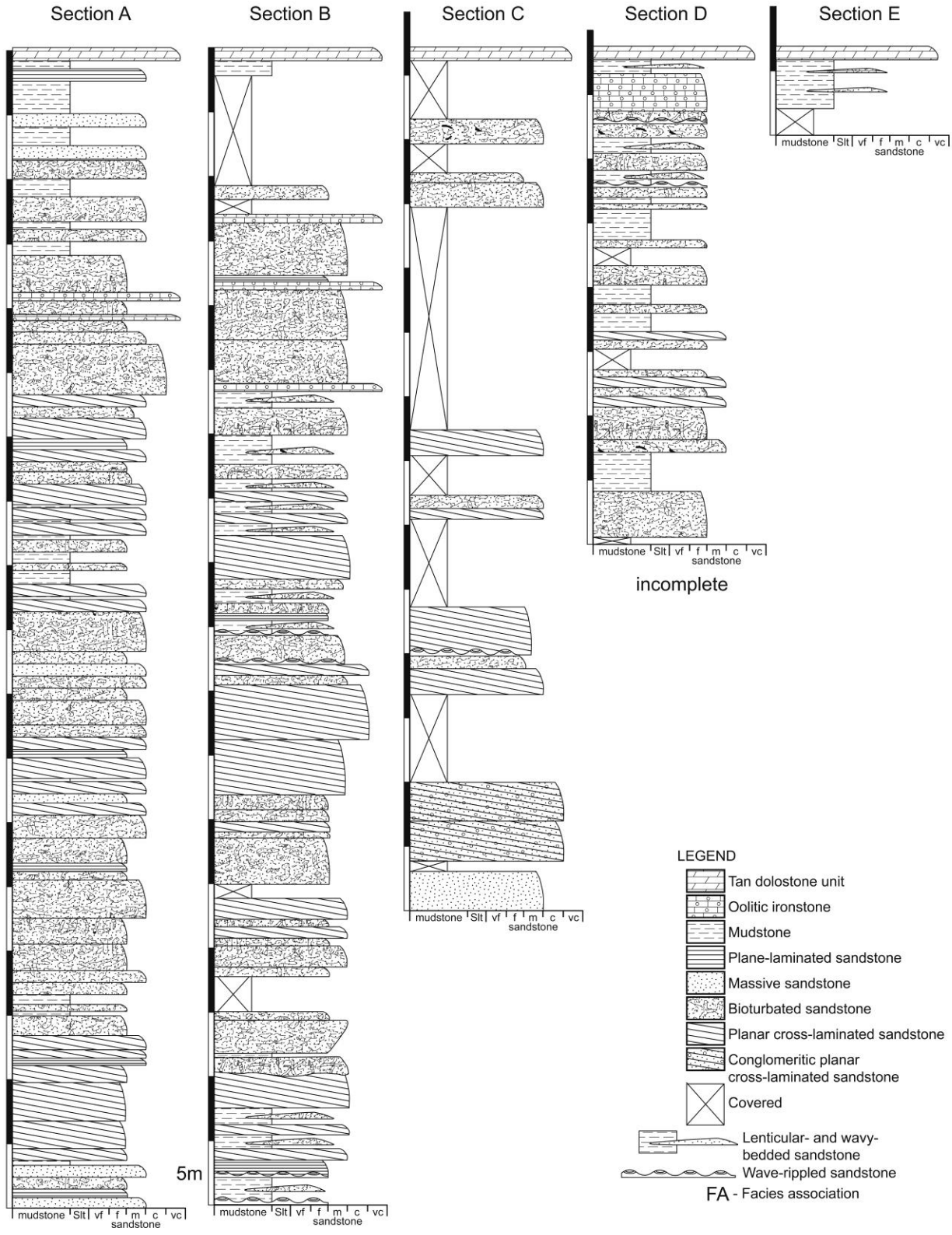
Section A
Section B
Section C
Section D
Section E
mudstone Slt vf f m c vc
sandstone
incomplete
5m
LEGEND
Tan dolostone unit
Oolitic ironstone
Mudstone
Plane-laminated sandstone
Massive sandstone
Bioturbated sandstone
Planar cross-laminated sandstone
Conglomeritic planar cross-laminated sandstone
Covered
Lenticular- and wavy-bedded sandstone
Wave-rippled sandstone
FA - Facies association

Figure 4:

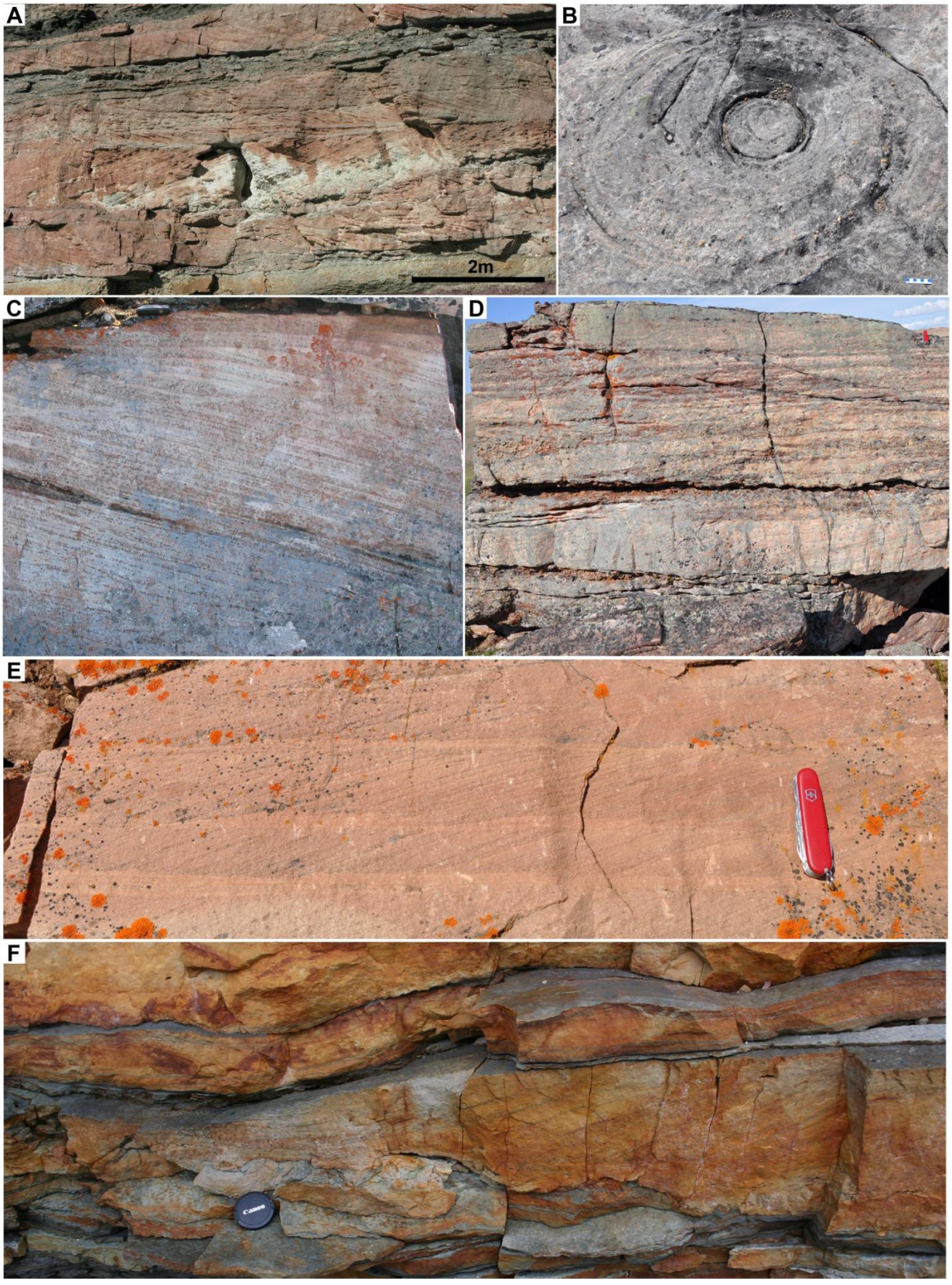

Figure 5:

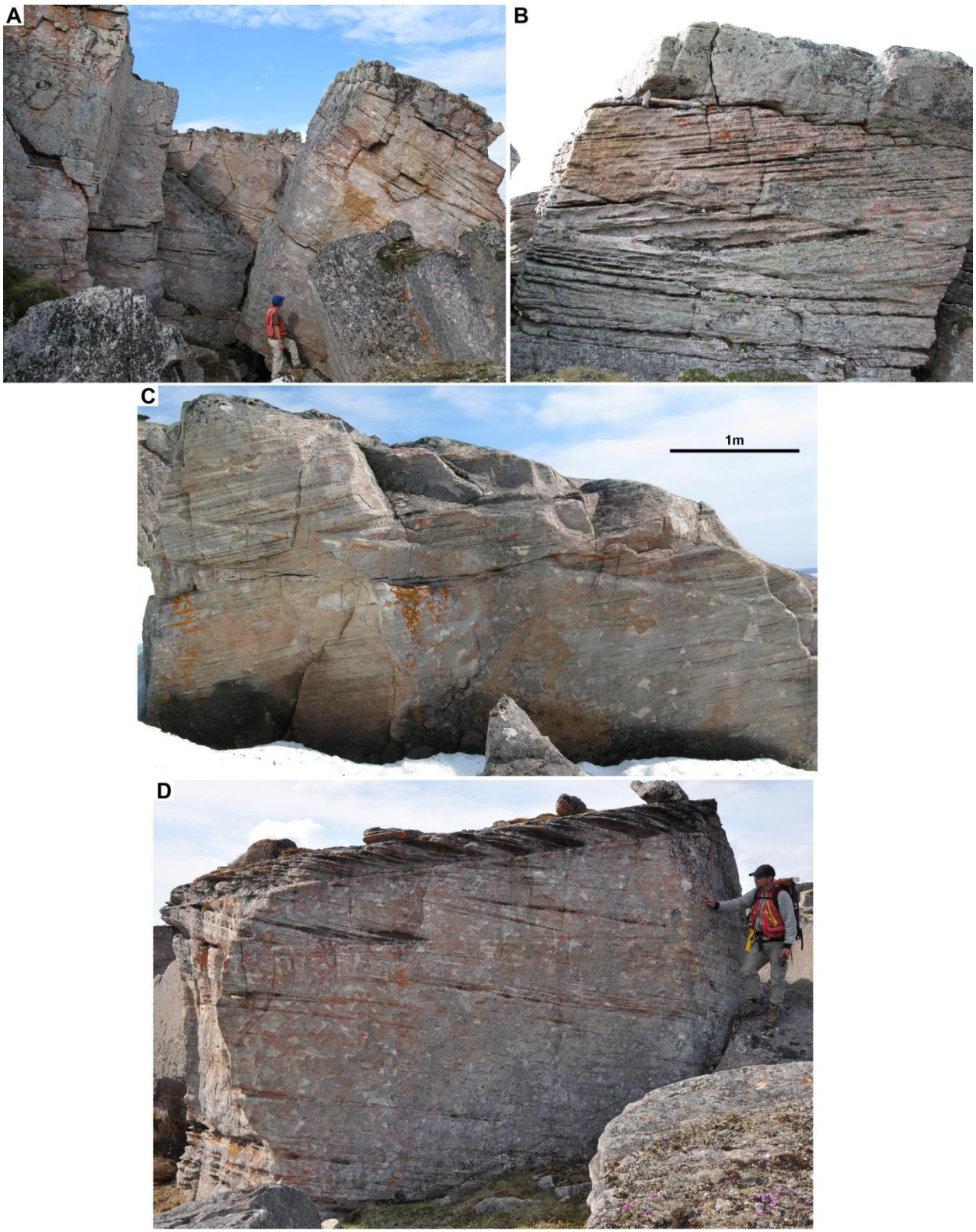

Figure 6:

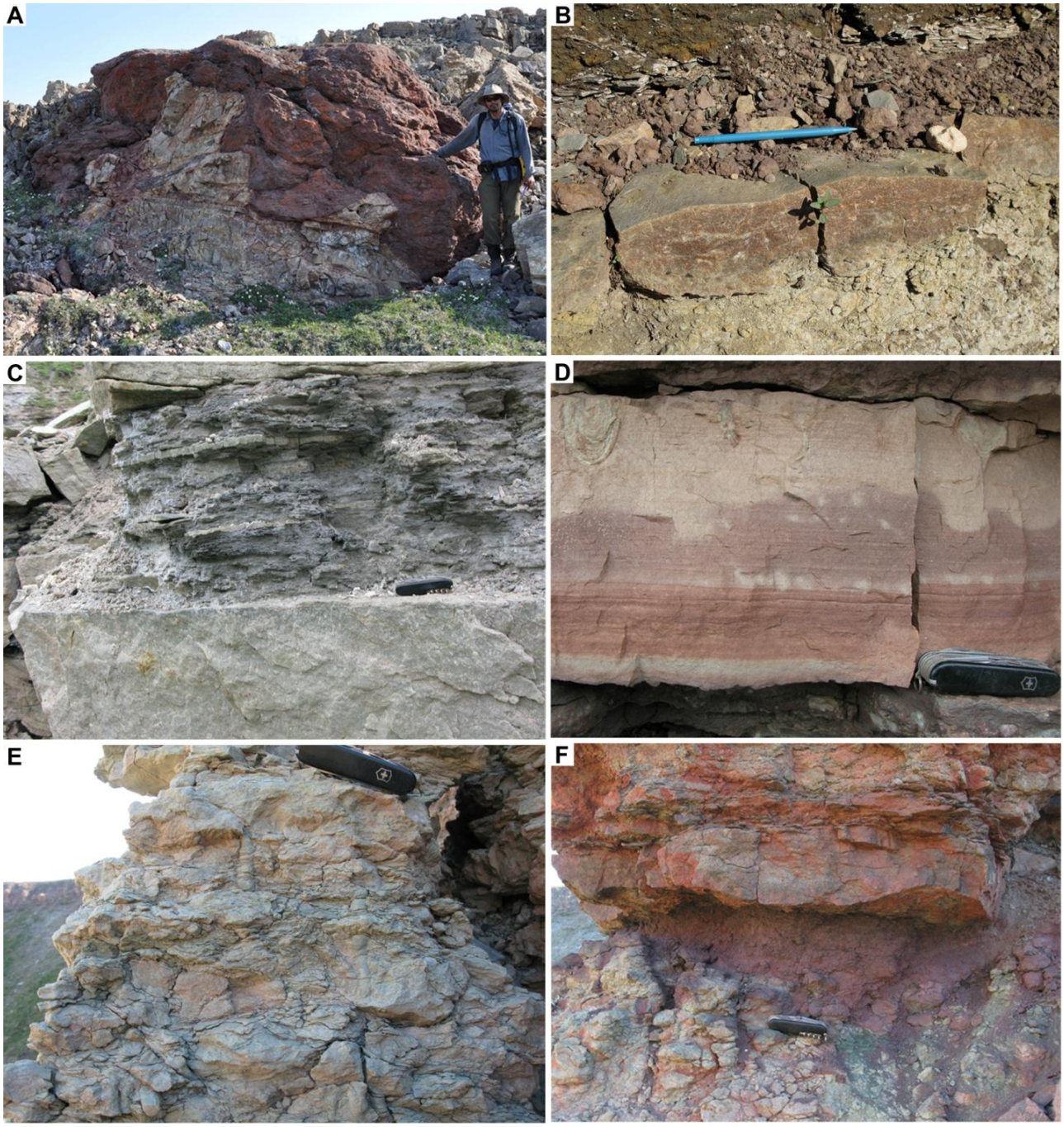

Figure 7:

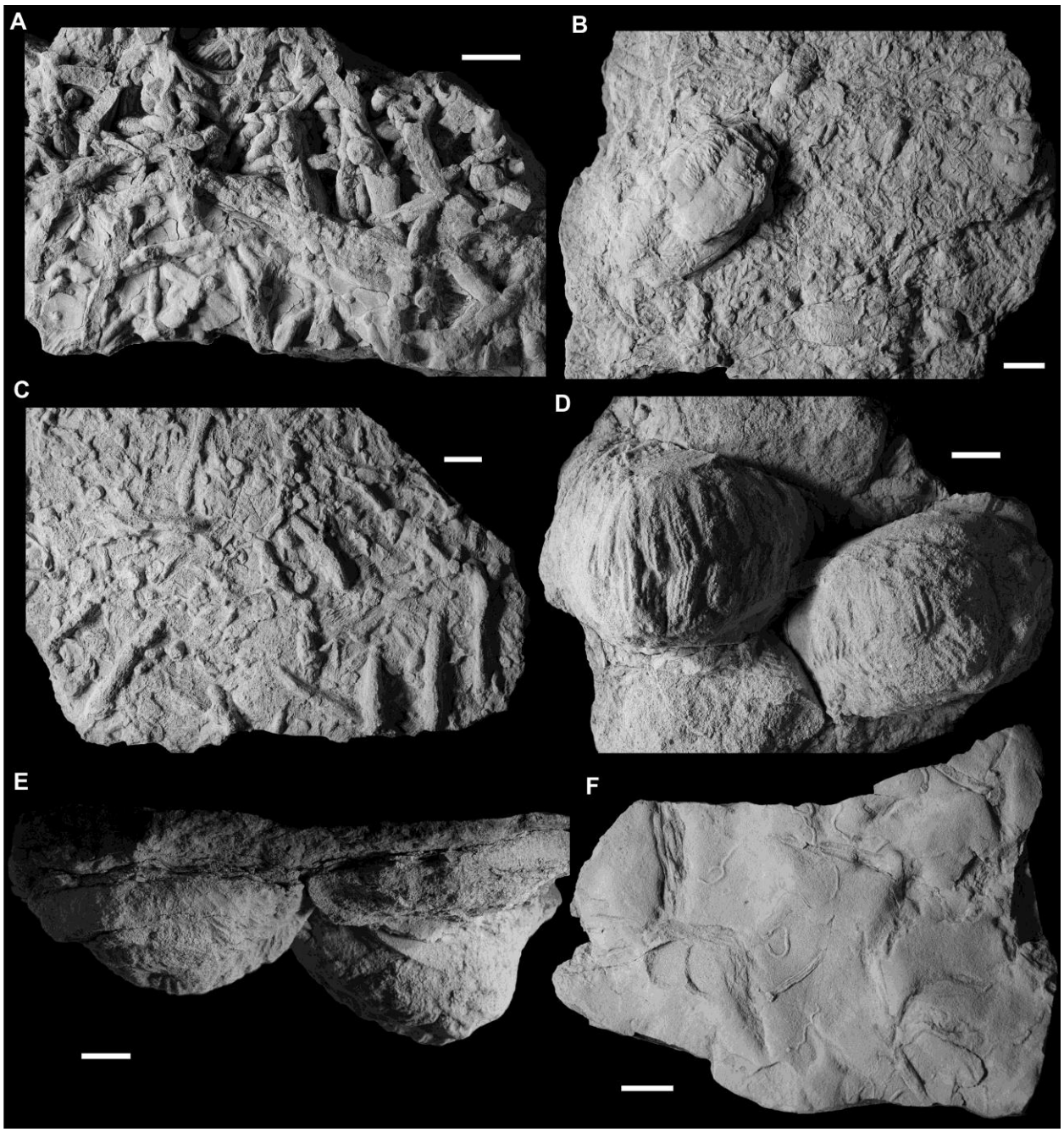

Figure 8:

Figure 9:

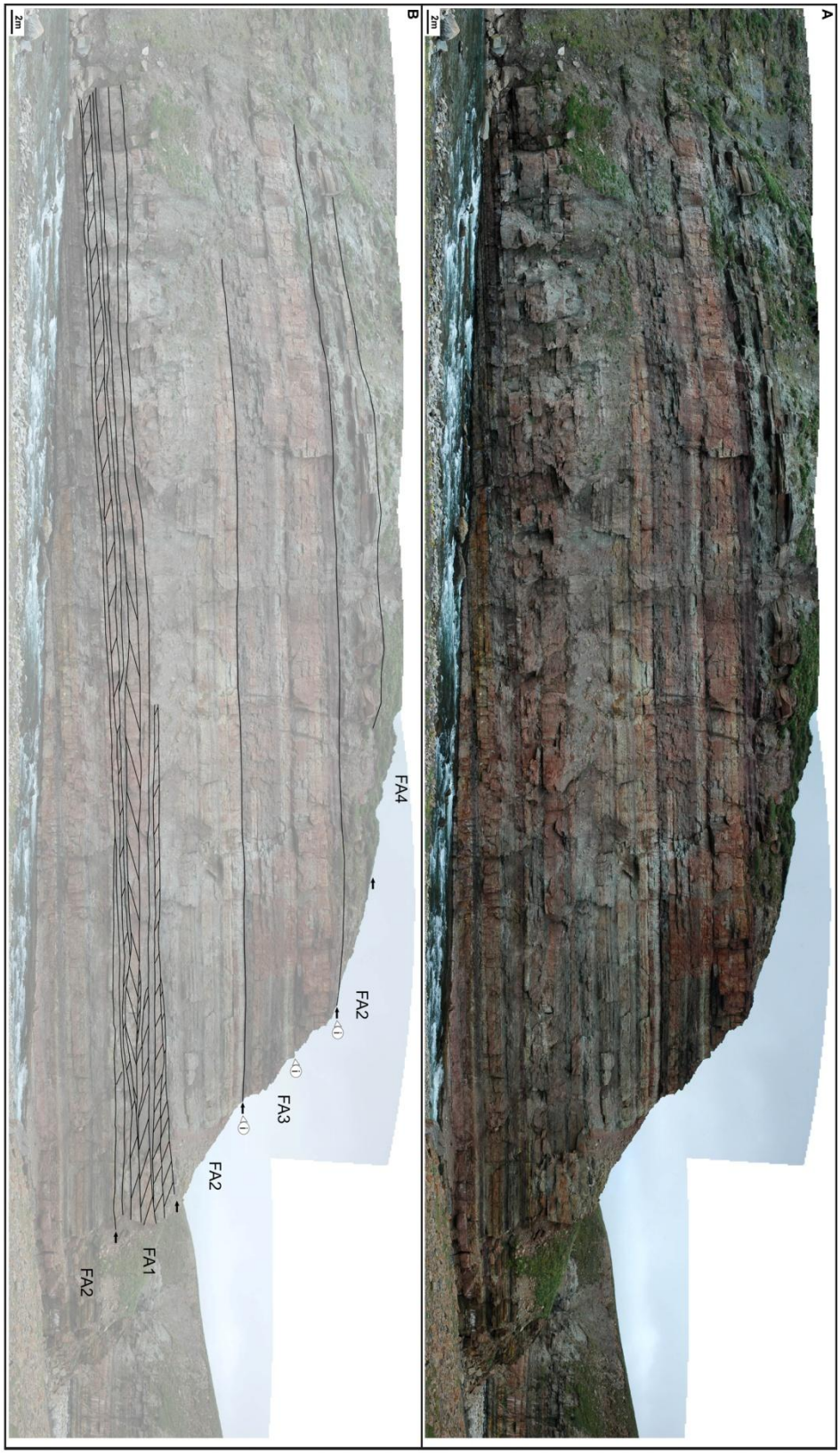

Figure 10:

Figure 11:

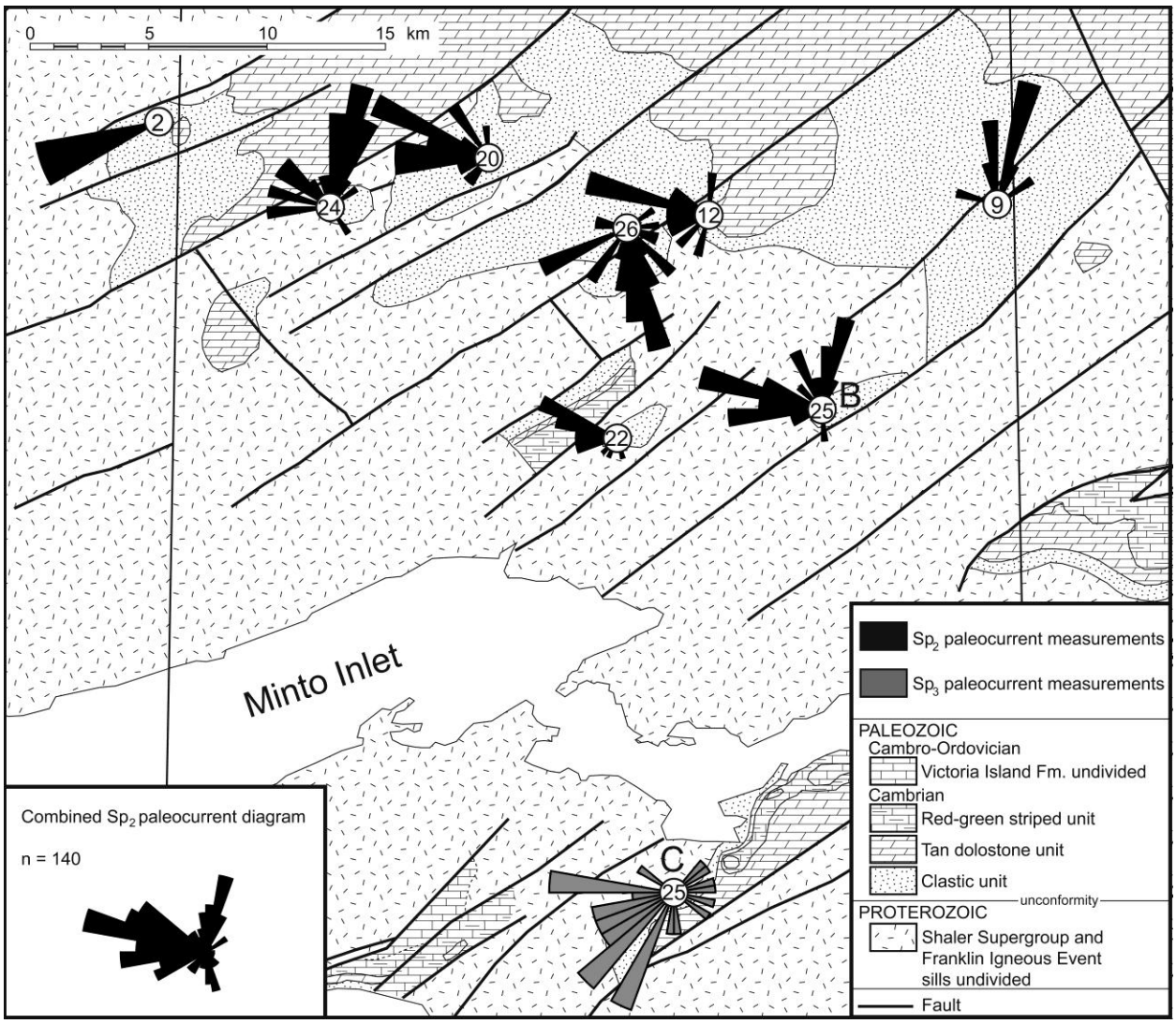
0
5
10
15 km
2
20
24
26
12
9
B
25
22
C
25
Minto Inlet
Combined Sp2 paleocurrent diagram
n = 140
Sp2 paleocurrent measurements
Sp3 paleocurrent measurements
PALEOZOIC
Cambro-Ordovician
Victoria Island Fm. undivided
Cambrian
Red-green striped unit
Tan dolostone unit
Clastic unit
unconformity
PROTEROZOIC
Shaler Supergroup and Franklin Igneous Event sills undivided
Fault

Figure 12:

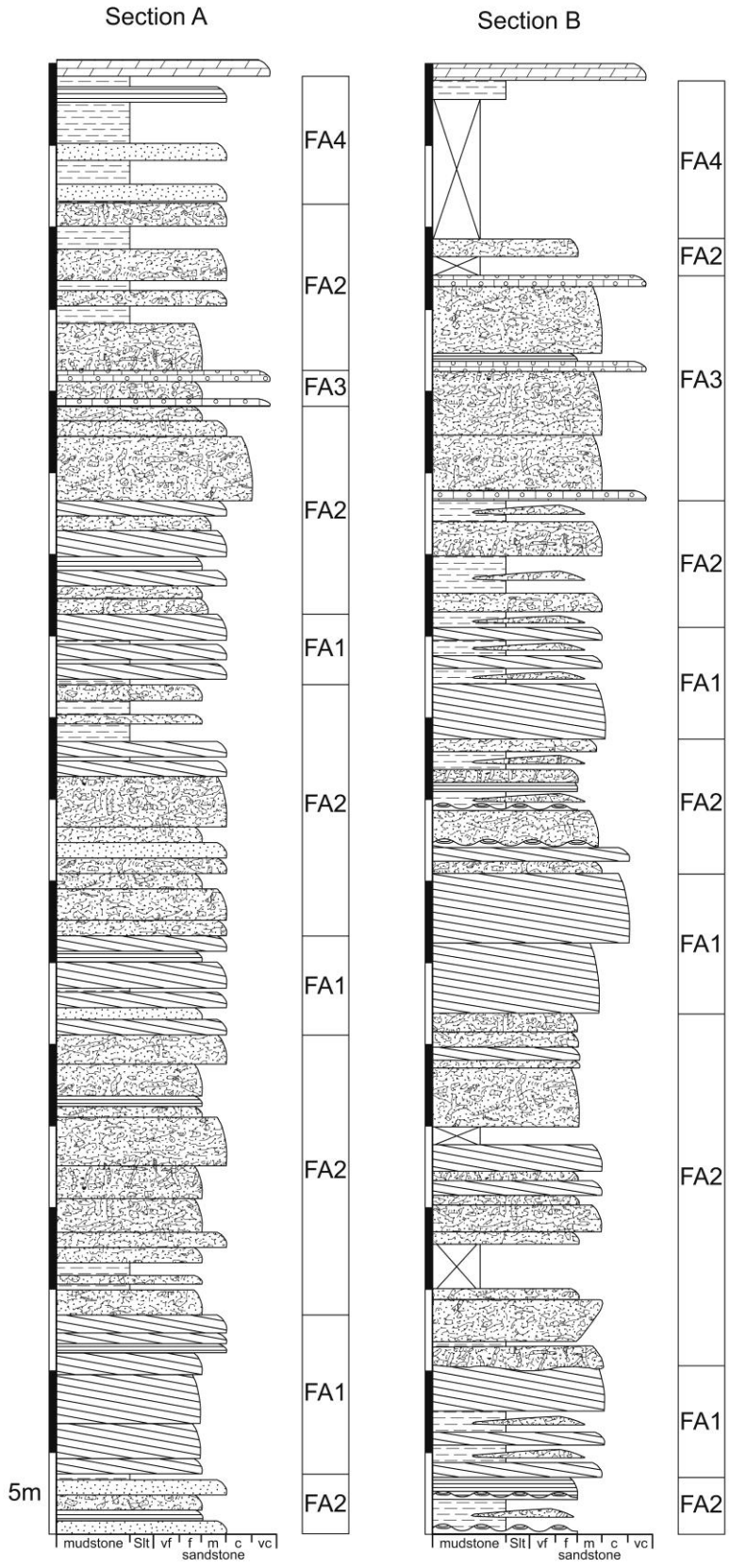
Section A
Section B
FA4
FA2
FA3
FA2
FA1
FA2
FA1
FA2
FA1
FA2
5m
mudstone
Slt
vf
f
m
c
vc
sandstone